CHALMERS
UNIVERSITY OF TECHNOLOGY

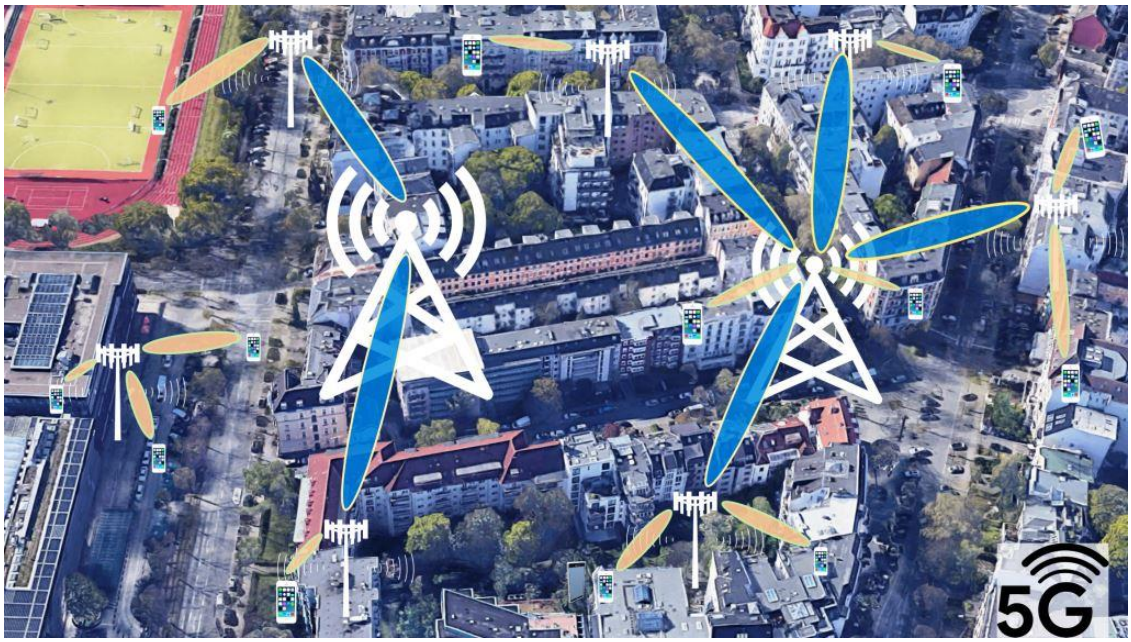

Power Control in Integrated Access and Backhaul Networks

Master's thesis in Communication Engineering

Haitham Babbili
Olalekan Peter Adare

DEPARTMENT OF ELECTRICAL ENGINEERING

CHALMERS UNIVERSITY OF TECHNOLOGY
Gothenburg, Sweden 2021
www.chalmers.se

Master's thesis 2021

Power Control in Integrated Access and Backhaul Networks

Haitham Babbili
Olalekan Peter Adare

CHALMERS
UNIVERSITY OF TECHNOLOGY

Department of Electrical Engineering
Wireless Systems Division
Communication Systems Group
Chalmers University of Technology
Gothenburg, Sweden 2021

Power Control in Integrated Access and Backhaul Networks
HAITHAM BABBILI, OLALEKAN PETER ADARE

Supervisor: Tommy Svensson, Department of Electrical Engineering, Chalmers

Co-supervisor(s):
Behrooz Makki, Ericsson Research
Charitha Madapatha, Department of Electrical Engineering, Chalmers

Examiner: Tommy Svensson, Department of Electrical Engineering, Chalmers

Master's Thesis 2021
Department of Electrical Engineering
Wireless Systems Division
Communication Systems Group
Chalmers University of Technology
SE-412 96 Gothenburg
Telephone +46 31 772 1000

Cover: Illustration of an integrated access and backhaul network in urban macro environment.

Typeset in LaTeX
Printed by Chalmers Reproservice
Gothenburg, Sweden 2021

Power Control in Integrated Access and Backhaul Networks
HAITHAM BABBILI, OLALEKAN PETER ADARE
Department of Electrical Engineering
Chalmers University of Technology

Abstract

The integrated access and backhaul (IAB) network is a novel radio access network (RAN) solution, proposed by the 3rd Generation Partnership Project (3GPP). IAB network is one of the interesting aspects of the fifth-generation (5G) RAN. The IAB networks thrives on the advantage of using all ranges of spectrum defined for the 5G new radio (NR) to interconnect the mobile and fixed access users to the network, and still bulk transmit their data towards the 5G core network. IAB networks may reduce the dependency on the optical fiber network and out-of-band frequencies for backhauling. However, there are inherent challenges that come with this approach. A possible constraint may be interference, which reduces the received signal quality. This, in turn, reduces the user data rate. Therefore, interference should be mitigated or canceled optimally. Using power control combined with adaptive beamforming, resource allocation and routing techniques may help to deploy efficient IAB networks, with higher spectral efficiency and better service coverage.
This thesis focuses on a power control solution in uplink communication within IAB networks. A power control solution may effectively reduce the effects of interference among all the transceivers and keep the network operating at a signal-to-interference-plus-noise-ratio (SINR) that is needed to guarantee mobile services. The solution is built on a genetic algorithm (GA), which offers reasonable solutions in multi-objective problem formulations. The performance of the solution is then evaluated using the service coverage probability. Service coverage probability is the probability of the event that the users are provided with a minimum data rate. First, a wireless network model is set-up using using millimeter wave characteristics. Then, a finite coverage area is built with randomly distributed users and statically positioned base stations with transmit power constraints, as proposed by 3GPP. Afterwards, a wireless access channel is modeled that takes into account the predominant channel constraints, where the duplexing mode is time division duplex (TDD). Finally, the SINR and transmit power of all mobile terminals (MT) are optimized at every epoch using the GA. Interestingly, the GA offers a proper convergent solution for power control in IAB networks. Furthermore, based on the various simulations and results, there is a possibility that IAB networks with a well implemented power control scheme can achieve a better service coverage probability in uplink communication, than non-IAB networks.

Keywords: 5G NR, Integrated access and backhaul, IAB, signal-to-interference-plus-noise-ratio, 3GPP, power control, uplink, service coverage probability, genetic algorithm, wireless backhaul.

Acknowledgements

First of all, our profound gratitude goes to Professor Tommy Svensson for giving us this rare opportunity to conduct the thesis. He offered his plethora of knowledge in supervising our work. He offered us a high degree of academic research freedom which enabled us to learn and re-learn satisfactorily. Your always friendly and professional approach is endearing. Without your help, the aim of the project would not have been actualized.

Secondly, we are indebted to Dr. Behrooz Makki from Ericsson. He was always available and down to earth in offering guidance from his wealth of experience on the practical solutions in 5G networks and beyond. You were motivating us consistently while offering words of advice at each stage. It would have been difficult to get this done without you. We thank you. Our deepest appreciation goes to Ericsson AB for their overall support and technical guidance. Concisely, without you offering this thesis work, we would not have seen the bigger picture and the various solutions that abound in the telecommunication industry.

Thirdly, we wish to show our gratitude to Charitha Madapatha. He was our co-supervisor and his earlier work on 5G and beyond complemented our project. Your simplified explanations, information, guidance and support were a huge advantage for us.

Furthermore, our sincere thanks go to the department of Electrical engineering, at Chalmers University of Technology. You made us see the engineering world from a unique prism of life. The enabling environment, opportunities and the general knowledge offered are top-notch.

Then, we would like to recognize the irreplaceable help from our families during our study. Your encouragement and resolute support gave us the needed strength to carry on. Without you, we would not have achieved a lot of our goals. We sincerely appreciate you.

Haitham Babbili and Olalekan Peter Adare, Gothenburg, June 2021

List of Acronyms

BS	Base Stations
CSI	Channel State Information
CU	Central Unit
DL	Downlink
DU	Distributed Unit
eMBB	Enhanced Mobile Broadband
FDD	Frequency Division Duplex
FHPPP	Finite Homogeneous Poisson Point Process
FWA	Fixed Wireless Access
GA	Genetic Algorithm
gNB	Next Generation NodeB
HARQ	Hybrid Automatic Repeat Request
HetNet	Heterogeneous Network
IAB	Integrated Access and Backhaul
ITU-R	International Telecommunication Union-Radio communication sector
KPI	Key Performance Indicator
LOS	Line-of-Sight
LTE	Long Term Evolution
mMTC	Massive Machine-type Communication
MBS	Macro Base Station
MIMO	Multiple-Input-Multiple-Output
mmWave	Millimeter Wave
NLOS	Non-Line-of-Sight
NR	New Radio
OFDM	Orthogonal Frequency Division Multiplexing
QAM	Quadrature Amplitude Modulation
QoE	Quality of Experience
QoS	Quality of Service
RAN	Radio Access Network
RAT	Radio Access Technology
RB	Resource Block
SBS	Small Base Station
SDM	Space Division Multiplexing
SINR	Signal-to-Interference-plus-Noise Ratio
TDD	Time Division Duplex
UE	User Equipment
UMa	Urban Macro
UL	Uplink
uRLLC	Ultra Reliable Low Latency Communication
VR	Virtual Reality
WDM	Wavelength Division Multiplexing
Wi-Fi	Wireless Fidelity
WiMAX	Worldwide Interoperability for Microwave Access
2G	Second Generation

3G	Third Generation
3GPP	3rd Generation Partnership Project
4G	Fourth Generation
5G	Fifth Generation

Contents

List of Figures

List of Tables

1

Introduction

1.1 Background and Motivation

Logically, the telecommunication network is divided into the access network, transport network, and the core network, [1]. The access network consists of wireless and wired resources that are used for delivering last-mile services to the users. In wireless access networks, services are mainly delivered via a base station (BS). The BS in a 5G network is referred to as the Next Generation NodeB (gNodeB or gNB), [2]. The transport network consists of all transmission media and technologies for backhauling and interconnecting all entities within the entire telecom network. Backhauling is usually achieved with optical fiber and point-to-point microwave links, [3]. The optical transport solutions are usually built on wavelength division multiplexing (WDM) and Carrier Ethernet. The core network is the decision layer of the network and without it, the network cannot offer any of the intended services. The core node of the 5G network is generally referred to as the 5GC. The 5GC handles interconnection of the sub-networks or clusters, address and mobility management of the user equipment (UE), session management, user or data plane management, policy control, authentication, network slicing and other unique functions. 5GC also hosts the major applications offered by the 5G network, [4], [5].

Historically, there is a growing trend in demand for wireless access solutions. Users and businesses need more flexibility and cheaper access to their mobile services. Fixed wireless access (FWA) is a viable approach to meet their wireless access demands. FWA is more cost effective as compared with fixed broadband last-mile access like optical fiber, [6]. Using optical fiber links for backhauling and node-to-node interconnection is reliable to a large extent, since it is immune to electromagnetic interference and can support Terabits per second data rates.

Conversely, fiber is expensive to deploy, and it may not be attainable to have it everywhere. Due to the local geometry and features in some locations, optical fiber installations may not be feasible. The cost of maintenance and replacement is also relatively high. Then, there are some governing policies in certain locations that do not allow installing new infrastructures for the use of optical fiber. Therefore, the other option in this case is FWA. FWA offers shared point-to-multipoint last-mile service delivery, unlike fixed broadband connections. It should be noted however that FWA uses the wireless channel which will have to contend with all the factors affecting the wireless signal. The varying characteristics of the wireless channel will

lead to varying service quality and data rates for the end users. The varying service quality also depends on the cell load, [6]. Additionally, the frequency band in use determines the coverage of the wireless service, as the transmitters are power limited. Low frequency bands have longer wavelengths and so have a better coverage than high band frequencies. Typically, wireless backhauling for FWA base stations require a different frequency band which comes at a cost of acquiring separate frequency spectrum for both wireless access and backhauling.

Moreover, the 5G wireless network is designed to offer high-rate data streams for everyone, everywhere, and at any time. 5G comes with a need for a higher channel bandwidth allocation for the radio access network (RAN). In order to support a higher number of devices per square kilometer, the network needs to be highly densified. Basically, point-to-point wireless backhaul links have always been designed based on line-of-sight (LOS) and non-standardized technologies utilizing high frequencies. With 5G in an urban area, the small base stations (SBSs) will be at the street level thereby creating a chance for non-line-of-sight (NLOS) in the backhaul links. Also, the access link, which previously was at low frequencies, is moving to millimeter wave (mmWave). The mmWave range was previously dedicated to backhaul links. Then, having non-standardized technologies in mmWave backhaul is no more reasonable, as it will conflict with the access links. These NLOS backhauling capabilities and the use of standardized backhauling are the main motivations for IAB networks. Of course, cost, flexibility, and low time-to-market are further motivations for both wireless backhaul and IAB networks.

3GPP has offered a multi-hop IAB network solution, with a distributed architecture. Here, each IAB node, or SBS, can be connected to the macro base station (MBS), referred to IAB donor, using the same frequency of the wireless access link. Using the same frequency for access and backhaul is called in-band backhauling. On the other hand, out-of-band backhauling is when the backhaul and access links operate in different frequency bands.

In brief, using IAB nodes will further improve the service coverage within a target area. Inherently, using in-band backhauling introduces more interference for the backhaul links, which may limit the service coverage probability and the actual data rate that the end-users can achieve. In this scenario, a well-known wireless communication solution is to define a proper network plan about the BS locations and power levels. However, network planning is an offline approach which does not factor in real-time channel realizations. If required, dynamic power control and rate adaptation may further improve the service coverage probability, [7], [8].

Power control aims to always have a specific minimum signal-to-interference-plus-noise ratio (SINR) at all times, irrespective of the channel conditions. Although, having the required minimum SINR may not be feasible at all times. On the other hand, rate adaptation, or rate control, aims to achieve an overall service availability as much as possible, by intelligently adjusting the modulation scheme and coding rate of the communication system, according to the prevailing channel conditions.

Power control is usually used in uplink communication, while rate adaptation is usually used in downlink communication, with fixed transmit power from the BSs.

1.2 Aim

The aim of the thesis work is to find an appropriate power control scheme for implementation in a 5G IAB network. The thesis also put into consideration various environmental factors and constraints that can limit the service coverage and performance of the 5G IAB network. The objective is to study IAB network performance in uplink communication and achieve the following:

- Identify realistic channel models for mmWave communication in IAB networks.
- Identify the appropriate power allocation schemes in IAB networks.
- Develop a simulator to evaluate the effect of power allocation in IAB networks.
- Carry out comparisons between a single macro-cell network and dual macro-cell network, with power allocation.

1.3 Thesis Contribution

The thesis tries to answer the following research questions in wireless communication with regards to 5G IAB networks.

- Why power control may be useful in IAB networks?
- Why is having an efficient power allocation algorithm important in IAB networks, like using genetic algorithm (GA)?
- What will be the impact of intra-cell and inter-cell interference on service coverage probability of IAB networks?
- What is the benefit of separating access links and backhaul links in IAB networks, based on time division duplex (TDD)?

1.4 Limitations

The thesis investigates power control for the 5G IAB networks in uplink communication. Simulations are carried out with models and parameters suggested by 3GPP for 5G RAN. The work is not based on real 5G network data. Also, the thesis will not study the possibility of having simultaneous transmission and reception in IAB networks. All simulations will be carried out on MATLAB. The simulations will not consider the 5G network in an end-to-end manner. The thesis is limited to finding a proper power allocation scheme for the uplink channel in the 5G IAB network.

1.5 Methodology

The thesis is based on a simplified spatial model of a 5G IAB network. The model factors in a couple of wireless environmental factors in a well-planned out RAN. The model consists of multiple UEs and statically positioned base stations (Macro and Small BSs), and assumes that only the MBS is connected by non-IAB backhaul,

e.g., fiber, towards the core network. Then, there are a number of SBSs or IAB nodes whose traffic are backhauled to the MBS using in-band communication. The model tries to maximize the SINR per node using a central GA solution. The GA will in turn try to maximize the service coverage probability, under the designed IAB conditions. The main measurement metric is the service coverage probability.

1.6 Previous Work

First, there are a couple of other related works based on 5G IAB network structure and coverage in downlink communication [9], [10]. In particular, their work provides the background about IAB network architecture and service coverage in downlink communication. Furthermore, a simulation of the 5G IAB network is made using the finite homogeneous Poisson point process (FHPPP) model which uses 28 GHz band, 1 GHz channel bandwidth and sets a minimum data rate of 100 Mbps per UE. Their work specifically compares service coverage with backhaul bandwidth of the IAB network.

Then, [11] investigates the actual number of IAB nodes that are needed for an optimum 5G IAB deployment. Their work simulates a resource scheduling scenario for 5G IAB using 28 GHz band with 1 GHz bandwidth, characterizing the transmission control protocol-internet protocol (TCP/IP) stack. Their work also identifies possible challenges in throughput and latency of the related 5G service.

Also, [12] discusses and evaluates the coverage extension improvement in 28 GHz band with IAB deployment in 3GPP Urban micro (UMi) scenarios. Their work compares IAB schemes with and without dynamic TDD interference using centralized scheduling. The simulation-based results show that a fully flexible IAB network can achieve around 60% gain in the uplink and 100% gain in the downlink, as compared with non-IAB deployment. Moreover, the scheme without dynamic TDD interference shows a good gain in downlink communication. The results point to the fact that achieving high spectral efficiency at the backhaul is important for the overall system performance.

Additionally, [13] investigates the power allocation problem for a proposed in-band self-backhaul scheme. The set-up works with multiple antennas with full-duplex communication at the BS, which enables the access and backhaul to work simultaneously within the same frequency band. An iterative algorithm is proposed to successively allocate the powers in the considered scenario so that the users' sum-rate is maximized, while taking into account the capacity limits of the backhaul link. Then, their work identifies cross-link interference and self-interference, or co-channel interference, as the major challenges that must be mitigated. The results show that the interference between the backhaul and the access networks of in-band self-backhauled networks is a major limiting factor to the overall system throughput, which can be alleviated using proper power allocation schemes. Moreover, resource scheduling is considered as a key to having an overall optimal solution.
Furthermore, [14] details the IAB network in an end-to-end manner, in line with

3GPP release 16 (Rel-16) proposal. Specifically, their work shows that the IAB network still has a half-duplex constraint, even though it can support space division multiplexing (SDM), frequency division duplex (FDD), and TDD.

Interestingly, [15] formulates a multi-hop scheduling problem to propose an efficient IAB network deployment. The work further stresses the need for a resource scheduler and proposes not having more than two hops away from the donor gNB. Reducing the number of hops is to lower the end-to-end network latency, while still achieving the required data capacity for access and backhauling.

On IAB network topology optimization, [16] looks into using GA formulations for both IAB node and non-IAB backhaul link distribution. The work makes a case for efficient routing in locations with severe availability constraints and high blockage densities. Therefore, load balancing the traffic across the network becomes important in order to improve the service coverage. The work also summarizes the recent Rel-16 approved solutions as well as the latest Rel-17 3GPP considerations on traffic routing in IAB networks. For a resilient RAN, mesh-based IAB networks are proposed.

Taking a look at future wireless networks, [17] investigates the use of a predictor antenna to boost the service performance in moving IAB networks. Mobility of either the transmitter or receiver, or both, results in variations in wireless channel conditions. The paper considers having a single antenna mounted on vehicles as a moving IAB node to boost service in both urban and rural areas, with backhaul supported by either terrestrial or satellite communication. Field trials shows that moving IAB nodes offers up to 50% improvement in backhaul throughput as compared to open-loop schemes.

Moreover, [18] studies the advantage of scheduling and data rate maximization in IAB networks. The work proposes a minimum throughput maximization algorithm for IAB networks. The model considers pathloss, directional beamforming, and antenna gain array of the BSs. The simulations are set-up to optimize resource scheduling of IAB nodes by maximizing the minimum throughput of the access links based on the revised simplex method. The results show that with IAB networks, there is a possibility to achieve a minimum throughput that out performs MBS only networks.

1.7 Thesis Outline

The thesis report is arranged to introduce the work and fully detail the work done. Chapter 1 introduces the thesis work. Chapter 2 gives the theoretical background and deployment overview of IAB networks. Chapter 3 explains system models used and the methodology. Chapter 4 covers the simulations and results. Chapter 5 offers the conclusions from the thesis work, while Chapter 6 lists the related future works on IAB networks, that could be of interest. Finally, all references and other sources of information used are listed.

2

Theoretical Background

2.1 5G New Radio

5G new radio (NR) is the newest radio access air interface of the 5G network. 5G NR offers a unified and more robust RAN than the previous technologies, such as second-generation (2G), third-generation (3G), and the fourth-generation (4G), [19]. It is specifically designed to support new generation services and various use cases like virtual reality (VR) and 4K/8K videos, [20]. Specifically, 5G NR offers a flexible bandwidth use with similar modulation schemes as 4G. The flexibility of 5G NR supports different access services in terms of coverage capacity, data rate, and latency requirements, [21]. Also, 5G NR comes with improved channel coding, waveform generation, massive multiple-input-multiple-output (MIMO), beamforming, network slicing, improved frame structures, hybrid automatic repeat request (HARQ), and duplexing, [5], [19]. The combination of all these makes it far superior to the previous technologies. Fig. 2.1 illustrates the 5G NR use cases.

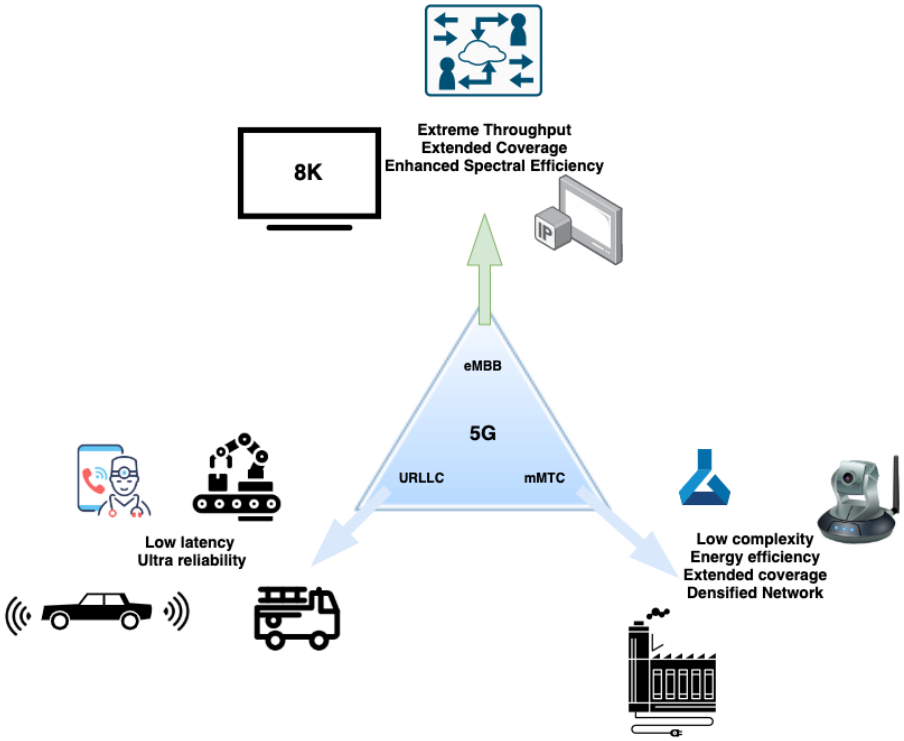

Figure 2.1: Illustration of 5G NR use cases. 5G NR services are classified as eMMB, URLLC and mMTC.

As a standard, 5G services are classified into three categories. These are enhanced mobile broadband (eMBB), massive machine-type communication (mMTC), and ultra-reliable and low-latency communication (uRLLC), [22].

5G promises improved user experience with a latency down to 1 ms, over the wireless channel, data rates of between 100 Mbps and 1 Gbps per UE, and Terabits per second data rate per square kilometer. There are on-going studies for 5G to support mobility of up to 300 km/h, [23]. Also, 5G NR uses orthogonal frequency division multiplexing (OFDM) technology, which is a widely used spectrally efficient wireless access technology. OFDM is already in use in IEEE 802.11 wireless fidelity (Wi-Fi), Worldwide Interoperability for Microwave Access (WiMAX), and 4G long-term evolution (LTE).

Going forward, the first resource needed to support the 5G network is the allocated frequency band. The frequency band determines how much channel bandwidth the RAN can support which is based on regulations. NR is licensed to operate both at low and high-frequency bands. The NR bands are further described as the sub-6 GHz, depicted as FR1 (0.45 GHz to 7.125 GHz), and the above 6 GHz bands, depicted as FR2 (24.25 GHz to 52.6 GHz), [5], [19], [32]. 5G offers flexible channel bandwidths of 50 MHz, 100 MHz, 200 MHz, 400 MHz, and where possible 800 MHz and more. The sub-6 GHz bands are already in use by various wireless technologies like 2G, 3G, 4G, WiMAX, Satellite communication, point-to-point microwave radios, and much more. Therefore, it has been a challenge to offer 5G NR higher bandwidth values in lower frequency bands. Interestingly, in the mmWave band, there is the possibility of being allocated any channel bandwidth partitions supported by 5G NR, ranging from 50 MHz to 800 MHz. Furthermore, the 28 GHz band is attracting interests across the telecommunication domain, [12], [13], [23].

Technically, the main requirements for achieving higher data capacity per square kilometer in the radio access networks are the allocated channel bandwidth, spectral efficiency and cell density, [7]. In communication design, the channel bandwidth directly relates to the symbol rate. Therefore, an increase in the channel bandwidth will lead to an increase in the symbol rate and eventually the data capacity per square kilometer, with other parameters held constant. Then, there is the spectral efficiency which is translated to the number of bits per symbol per Hertz. Modulation and coding schemes are introduced to improve the spectral efficiency, [7].

Interestingly, 5G NR uses the same modulation as the 4G LTE network, with 256 QAM being the highest commercially for now, [21]. Moreover, 5G still offers the possibility of having a modulation scheme of up to 1024 QAM and 4096 QAM respectively, [24]. Then comes the cell density within a specific area. Every wireless BS has a maximum communication capacity in terms of data rate and the number of users that can be supported at an instant. If the number of BSs can be increased within a defined service coverage area, without having undue signal degradation, then the overall data capacity per square-kilometer will be greatly increased.

Mostly, these BSs are interconnected using out-of-band microwave backhaul or optical fiber. Out-of-band communication comes at an extra cost to the service providers, which needs to be reduced. Apart from fading, signal blockage, and shadowing, one major challenge in wireless communication is the interference from other transmitters located nearby. Blockage and shadowing are related to the local obstructions to the LOS path of the signal, while fading is due to variations in wireless channel conditions during communication. Since wireless communication is based on unguided media, interference in the wireless space cannot be totally controlled.

Furthermore, interference is additional noise contribution to the communication system. Interference may be prevented from reaching the receiver by controlling it at the transmitter side, or try cancelling it at the receiver side (or a combination of these). Interference can be co-channel interference, which is due to devices that are near and using the same frequency for communication. There is also adjacent channel interference which is due to devices using very close frequency bands. Higher cell densification within an area in 5G networks will further increase the interference. Invariably, the increase in the interference level within a targeted coverage area will decrease the signal quality, which further reduces the achievable data rate. Interference then becomes a challenge that must be controlled. Therefore, the SINR at the BS and achievable service coverage probability are important network key performance indicators (KPI) to study.

2.2 5G IAB Network Structure

Fundamentally, taking a BS as a reference, the transmission to the UE is called downlink (DL) communication. Conversely, the UE transmission back to the BS is called uplink (UL) communication. Simultaneous DL and UL is called full-duplex, while without simultaneous communication, it becomes a half-duplex system. Typical duplexing modes in wireless communication are FDD and TDD.

In FDD, specific frequency bands are divided into two frequency parts dedicated for DL and UL, which are then separated by a guard band in frequency to prevent transmitter-receiver interference. On the other hand, TDD offers UL and DL with the same frequency band, but in different time slots separated with guard times. There are also a few time slots, that are dedicated for synchronization (sync) of the entire communication between the UE and the BS. TDD comes with a half-duplex constraint, [7]. Fig. 2.2 illustrates the difference between FDD and TDD. Then, Fig. 2.3 is a simplified description of UL and DL communication with respect to the BS.

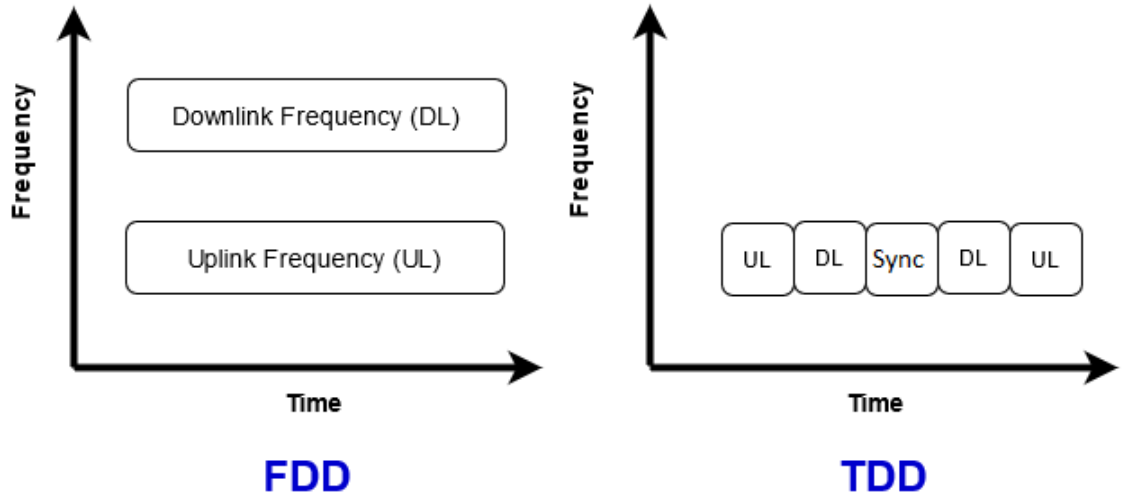

Figure 2.2: Illustration of FDD and TDD. Duplexing is based on time-frequency allocation for UL and DL.

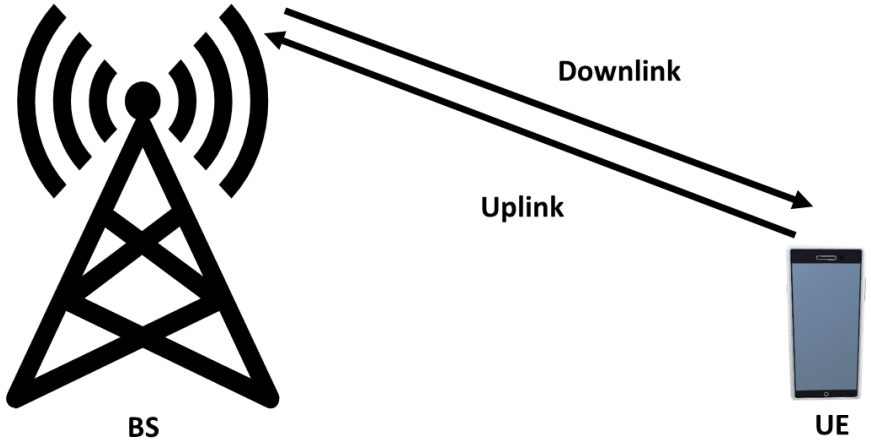

Figure 2.3: Illustration of UL and DL Communication. The BS is taken as a reference point for UL/DL illustration.

In IAB networks, BSs share the bandwidth resources between the UL/DL communication for the UE and the transport towards the 5G core network. The IAB network offers the use of distributed BSs where one can be the MBS, functioning as the donor BS, and a couple of other BSs, called SBS or IAB node, that depend on it for communication resources. The SBS will help extend service coverage area and availability within a targeted area. The SBS is not just a repeater station; it is a BS that depends on the MBS for frequency spectrum to backhaul the UE access traffic towards the core network, [10], [11], [25]. Without backhauling, the RAN is

incomplete. Backhauling is therefore critical in building a functional RAN. In this report, SBS and IAB nodes are used interchangeably.

Figure 2.4 is an illustration of the 5G IAB network. There is one MBS, i.e., IAB donor, with four SBSs, i.e., IAB nodes, connected to it via wireless backhaul links. The MBS is directly connected to the 5GC via non-IAB backhaul, e.g., optical fiber, and both the MBS and the SBSs are offering wireless access connections to the UEs. Eventually, all the data capacity within the service coverage area of the MBS is dependent on non-IAB backhaul, e.g., optical fiber, to connect to the 5GC. Moreover, all the SBSs and UEs within this service coverage area will be sharing the channel bandwidth that is allocated to the MBS. The MBS may connect to multiple SBSs and the SBSs may support multiple UEs. In general, IAB networks support an arbitrary number of hops from the MBS to the last-mile UE. The MBS, by virtue of the antenna design, supports massive MIMO. The narrowness of the beams from the MBS and SBSs in the downlink direction depicts beamforming towards specific SBSs and UEs. Based on the considered resource allocation strategy, a fraction of the channel bandwidth will be used for the access link, and the other bandwidth part will be used by the backhaul links.

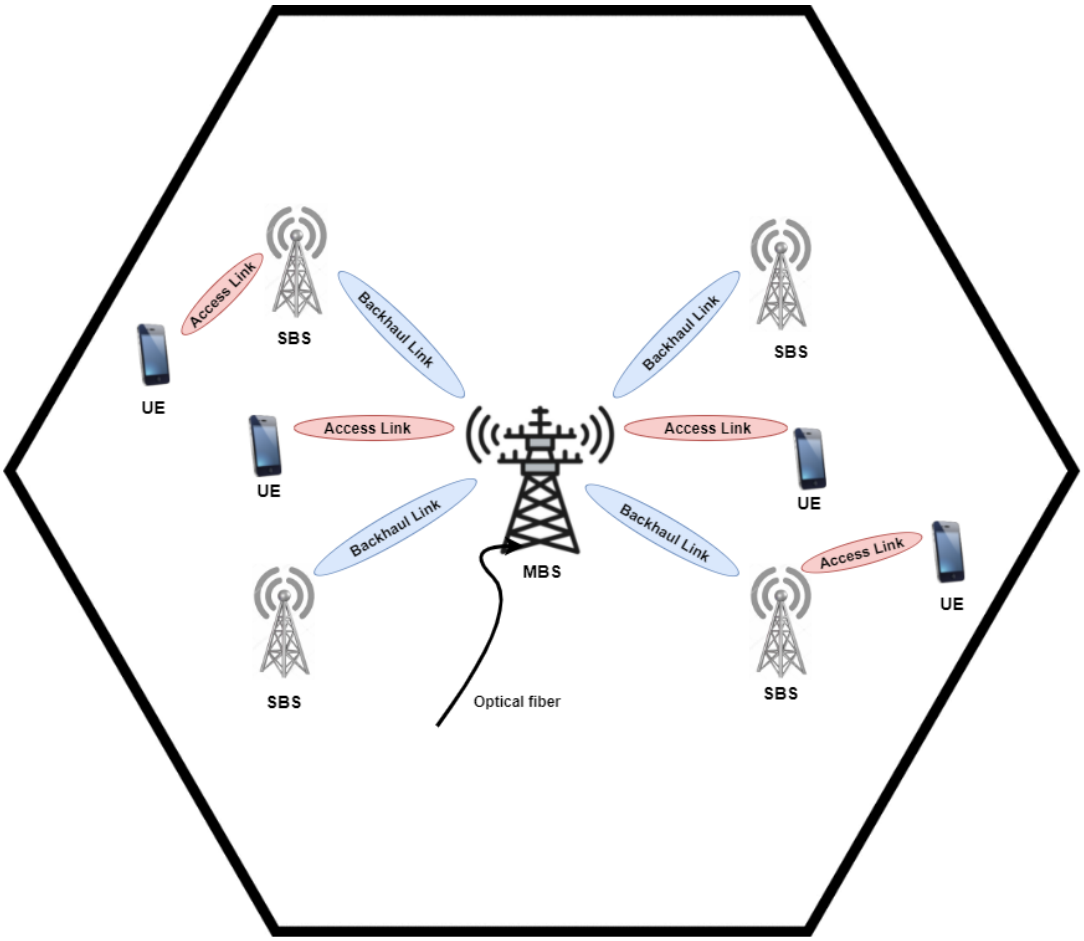

Figure 2.4: Illustration of 5G IAB network. There is one central MBS and four other SBSs depend on it for backhauling.

Table 2.1: 5G NR numerologies [26], [27].

Numerology (μ)	Sub-carrier spacing (kHz)	Slot Duration (ms)	Bandwidth (MHz)
0	15	1	50
1	30	0.5	100
2	60	0.25	200
3	120	0.125	400
4	240	0.0625	400, 800

Furthermore, an IAB network with a long chain of dependent SBSs may increase the end-to-end latency and cause backhaul congestion. High latency is an unwanted effect in IAB networks. Although, it is theoretically possible to have multiple hops, it is suggested to limit the number of hops in the IAB network to 2, [16]. Also, since the access and backhaul will be sharing the same frequency spectrum, then cross-link interference will be present. Cross-link interference is when BSs interfere with one another because they transmit and receive in the same spectrum and at the same time. Therefore, TDD is a viable option but it comes with a half-duplex constraint, in order to reduce interference. With TDD, the UEs are constrained to only periodic transmission and reception, which results in a lower capacity when compared with FDD. There are ongoing studies on how to achieve simultaneous transmission within IAB networks, [25].

Practically, 5G NR is based on OFDM using closely packed modulated sub-carrier signals, [26]. Each sub-carrier has its own bandwidth, or sub-carrier spacing (SCS). SCS is also referred to as NR numerology. NR offers various SCS values ranging from 15 kHz, 30 kHz, 60 kHz, 120 kHz, up to 240 kHz, [26], [27]. SCS of 120 kHz and 240 kHz are suggested for FR2 mmWave bands, because they can easily support 400 MHz and 800 MHz channel bandwidth respectively, [26]. A finite number of contiguous sub-carriers are then made into resource blocks (RB). One RB is defined as 12 consecutive sub-carriers in the frequency domain. Also, RB is the smallest time-frequency resource that can be allocated to a UE in OFDM systems. Therefore, the wireless BS will support a finite number of RBs based on the allocated channel bandwidth, [26]. Table 2.1 shows the 5G NR numerologies in this context. Then, Fig. 2.5 shows how RBs are shared between access and backhaul links.

Both the MBS and SBSs are capable of independently administering the channel bandwidth. Since only the MBS has a non-IAB backhaul, e.g., an optical fiber connection, towards the core network, then the SBSs must depend on the MBS for their backhaul bandwidth. Certain RBs are used for the interconnection between the MBS and the SBSs, which becomes the backhaul link for the SBSs. Then, other RBs can be used by the UEs to access the network. By the RBs sharing approach, the MBS can serve both UEs and SBSs at the same time. The access traffic from the UEs connected to an SBS will have to be switched from the RBs used in the access link to the RBs used in the backhaul link. Fig. 2.5 depicts all of these in context.

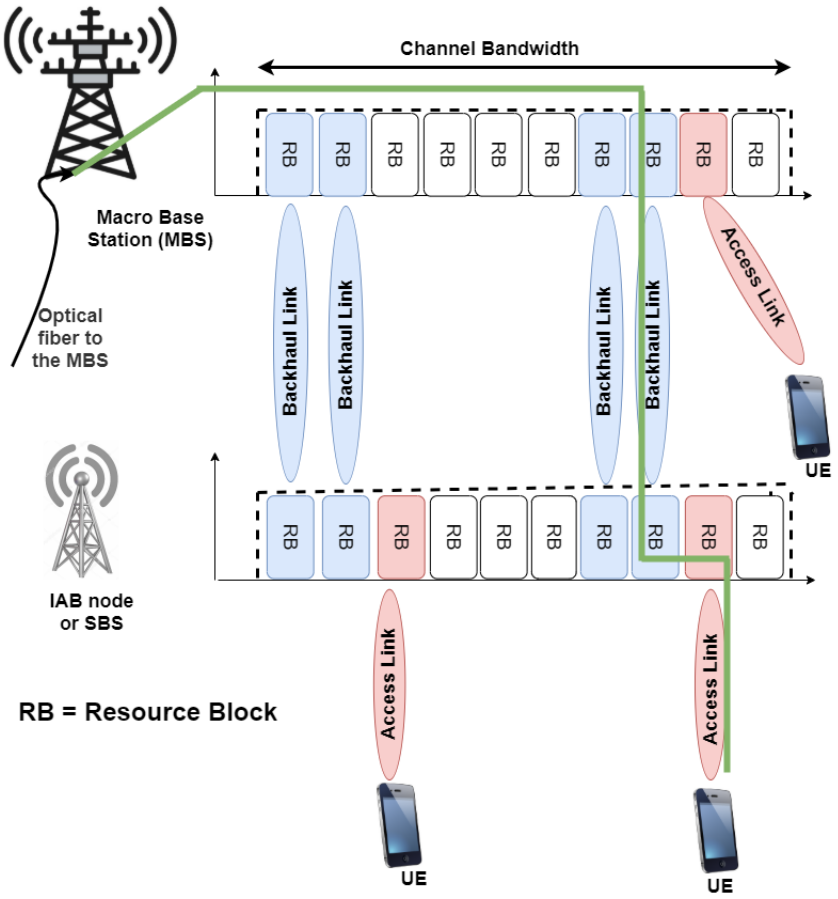

Figure 2.5: Resource sharing between MBS, SBS and UE. From [29]. Reproduced with permission.

2.3 Structure of IAB Nodes

The 5G NR structure, as standardized by 3GPP, supports a distributed architecture, [30]. The traditional deployment from 2G, 3G and even 4G LTE basically offers one MBS per location. However, the architecture of the BS in 5G has been separated into a central unit (CU) and a distributed unit (DU). IAB donor, i.e., MBS, is CU and DU combined, while the IAB nodes, i.e., SBSs, are mobile terminal (MT) and DU combined. The MT has similar functionalities as a UE. The MBS can support a finite number of SBSs within a specified location. Also, each of the IAB node has a finite number of UEs that can be supported at an instant. The CU/DU and DU/MT model is illustrated in Fig. 2.6.

2.4 The Role of Power Control in IAB Networks

Power control in wireless communication is a solution deployed to control the transmit power of the UEs in order to achieve an overall efficient communication system. Also, power control is an intelligent approach to reduce the power consumption of

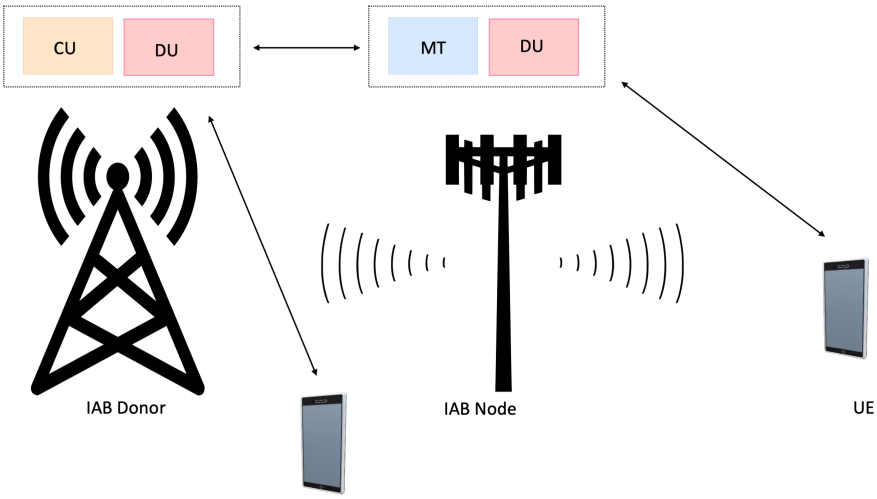

Figure 2.6: The Architecture of SBS/IAB nodes.

a transceiver device, which can either be a UE or a BS. In uplink communication, power control reduces the UE power consumption and the interference (inter, intra and co-channel interference), thereby increasing the service coverage probability, while reducing the outage probability. Typically, the more the interference power, the lower the SINR at the receiver, and the lower the achievable data rates, [13], [14]. Interestingly, to achieve high data rates in wireless communication comes at the cost of transmit power and SINR, irrespective of the channel noise and interference. A power allocation scheme tries to achieve the baseline SINR requirement, by dynamic transmit power assignment to the UEs irrespective of the prevailing channel conditions. Furthermore, power control is an important approach in maximizing cellular network capacity, by increasing the number of UEs that can be serviced within an area. Power control also helps to protect the BS receiver's circuit from power overload, which can damage the entire transceiver system.

In mobile communication, UEs are randomly distributed due to their mobility. Due to their mobility, the UE transmit power requirement varies per location and time. Power control is necessary to keep the power levels down based on global telecommunication regulations. Practically, all transmitters are power limited. Generally, UEs are classified into transmit power classes, [28].

Typically, users that are closer to the BSs transmit lower power than users that are far off. The UEs transmit at lower power because the magnitude of the pathloss is distance dependent, i.e., pathloss grows with distance away from the target BS. Controlling the power level of the UEs will help create a balanced received power level at the BS. Fading effect in the channel is also mitigated with power control. IAB networks bring the BSs closer to the users, thereby reducing their transmit power requirement and improving the users' experience.

3

System Model

3.1 Model Set-up

The system model considers an all-outdoor urban environment. The model supports a finite number of MBSs, SBSs and UEs. Fig. 3.1 shows the model set-up.

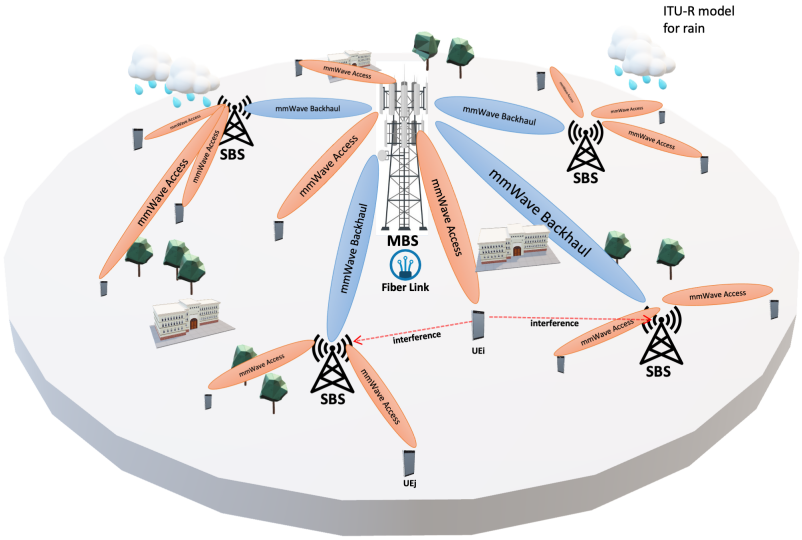

Figure 3.1: Schematic diagram of the system model of an IAB network.

The IAB network model in Fig. 3.1 is deployed to support a maximum of two hops from the MBS. The model supports $\boldsymbol{E}$ number of UEs that are randomly distributed within the specified coverage area of radius $\boldsymbol{r}$. The UEs are randomly distributed using the FHPPP approach, [11]. Also, there are M number of SBSs in fixed locations within the coverage area. Only the MBS_j has a non-IAB backhaul, e.g., fiber connection, that backhauls all traffic towards the core network. Two specific network arrangements are considered, (i) one MBS associated with a finite number of stationary SBSs, and (ii) two MBSs associated with a finite number of stationary SBSs each, in adjacent macro cells, in order to investigate inter-cell interference. The wireless channel is modeled to include the effects of shadowing, interference, pathloss, fading and rainfall. For the uplink, the SBSs and UEs are power-limited. The transmit power values are taken from 3GPP standard reference document, [30].

There is an arbitrary RB scheduler that governs the communication among the MBSs, SBSs and UEs.

Table 3.1: Definition of simulation parameters.

Parameter	Definition	Parameter	Definition
r	Cell radius	BW	Bandwidth
E	Total number of UE	E_m	Number of UEs that met minimum requirement of the service
M	Number of SBS	BW_{RB}	Bandwidth for one resource block
d_{2D}	2D distance	T_0	Thermal noise
d_{3D}	3D distance	U	Set of UE in coverage area
P_{EIRP}	Effective Isotropic Radiated Power	Gr	Receiver gain
α	Path-loss exponent	c	Speed of light
σ	Shadowing loss	CH	Channel capacity
P_t	Transmission power	RB_s	Number of resource block
P_r	Received power	E_{AccessUE}	Number of user related to access link
RCV	Receiver sensitivity	Γ	Polarization coefficient
L	Path-loss	k	Polarization coefficient
RB	Resource block	ϕ	Fading effect
R_b	Data rate	E	Number of UE
γ_R	Rain losses	Z	Set of SBS in coverage area
d_{BP}	Break point distance	N_0	Total noise
f_c	Carrier frequency	N_f	Noise figure
h_{BS}	Base station Height	SCS	Sub-carrier spacing
h_{UE}	UE height	h'_{UE}	Effective height for UE
h'_{BS}	Effective height of the base station	β	The percentage of the bandwidth resources
N	total number of iteration	K	Number of first iteration group in GA
S	Number of second iteration group in GA	V	Third number of iteration in GA
X_I	In-phase channel realization	X_Q	Quadrature channel realization
A	Set of associated UEs	W	Set of associated SBSs
d_0	Reference distance	ρ	Service coverage probability
R	Rain rate	t	Time
I	Interference	$SINR$	Signal to interference plus noise

The following are the general assumptions made for our work.

- An OFDM multi-access solution with a TDD duplexing option.
- A central TDD scheduler governs the communication of the base stations and UEs.
- MBS has 3 sectorial antennas, at 120 degrees each for a complete 360 degree coverage per base station, [31].
- The frequency band is 28 GHz, and the allocated channel bandwidth is 400 MHz (27.8 GHz to 28.2 GHz), [5].
- UEs can use different RBs per time slot, since they are assumed to be mobile and the wireless channel characteristics vary from time to time.
- The transmit power of the UE and SBS is taken as the effective isotropic radiated power (EIRP). EIRP is the transmit power plus the antenna gain, in decibel scale.
- Periodic access to channel state information (CSI) is available at the UE, SBS and MBS.
- The power control problem is treated as a multi-objective optimization problem.

3.2 Channel Modelling

3.2.1 Received Power

The received power at either the MBS or SBS is modelled as:

$$P_r = P_t + G_t + G_r - L - \sigma - \gamma_R - \phi. \tag{3.1}$$

Here, P_t is the transmit power, G_t is the gain of the transmitter, G_r is the gain of the receiver, L is pathloss, σ is shadowing loss, γ_R is rain loss, ϕ is the channel fading effect. All values are in dB. In our work, the transmit power values used are EIRP 3GPP defined values, where P_{EIRP} is expressed as

$$P_{\text{EIRP}} = P_t + G_t. \tag{3.2}$$

3.2.2 Pathloss and Shadowing

Pathloss accounts for a significant amount of signal attenuation in wireless communication. Pathloss depends on the distance between the transmitter and receiver, as well as the operating frequency band. The attenuation of the signal due to pathloss is distance dependent, [7]. A 3GPP UMa model is selected for the pathloss and shadowing, [33]. The model factors in the height of the MBS, SBSs and the UEs. It is viewed that the base stations are at a height higher than the UEs, with their antennas slightly down tilted towards the ground. The UMa pathloss model is represented in Eq. (3.3)

$$L = 32.4 + 10\alpha \log_{10}(d_{3\text{D}}) + 20\log_{10} f_c - 10((d_{\text{BP}}^{'})^2 + (h_{\text{BS}} - h_{\text{UE}})^2). \tag{3.3}$$

Here, L is the total pathloss in dB, and α is the pathloss exponent. d_{3D} is the 3D distance calculated using trigonometric equation, which is the LOS distance from the top of any UE to the top of the MBS. 2D distance is the horizontal distance from the MBS to a UE. Also, f_c is the carrier frequency, in GHz.
The pathloss exponent is related to the signal blockage, either in LOS or NLOS use cases. The relationship between pathloss and pathloss exponent can be expressed as in [10],

$$L = \begin{cases} r^{\alpha_L}, \text{for LOS.} \\ r^{\alpha_N}, \text{for NLOS.} \end{cases} \tag{3.4}$$

Then, h_{BS} is the height of the base station, and h_{UE} is the maximum height of the UE.
Also, $d_{BP}^{'}$ is the break point distance determined by the relationship in the Eq. 3.5

$$d_{\text{BP}}^{'} = \frac{4 * h_{\text{BS}}^{'} * h_{\text{UT}}^{'} * f_c}{c}. \tag{3.5}$$

Here, $h_{\text{BS}}^{'}$ is the effective antenna heights of the base stations, $h_{\text{UT}}^{'}$ is the effective antenna heights of the UE, and c is the speed of light in vacuum, estimated as 3 * 10^8 m/s. Fig. 3.2 illustrates the $d_{2\text{D}}$ and $d_{3\text{D}}$ distances.

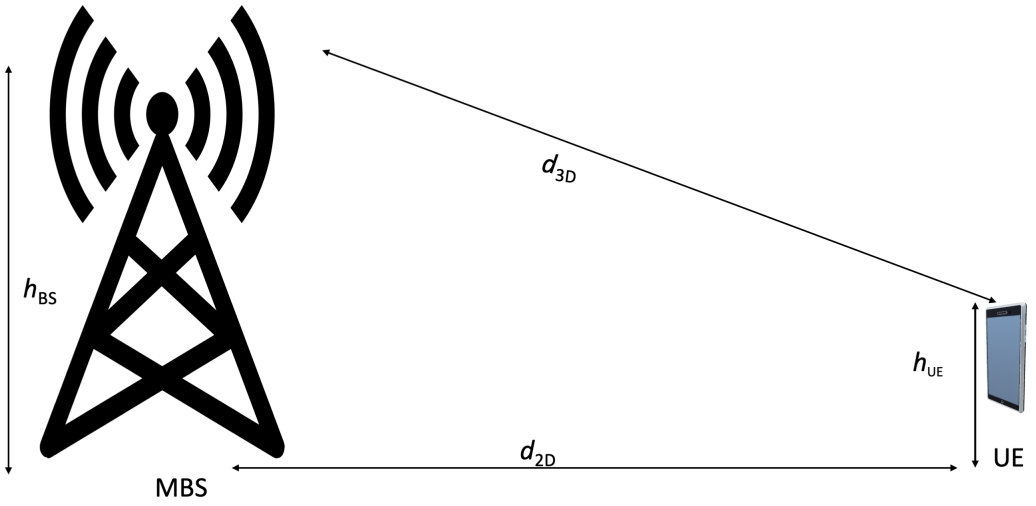

Figure 3.2: Illustration of d_{2D} and d_{3D} distances. From [33]. Reproduced with permission.

Shadowing is signal attenuation due to obstructions in the LOS path between the transmitter and the receiver. The magnitude of shadowing is proportional to the length of the obstacle. The common shadowing model is log-normal, i.e., ratio of transmit power to received power in linear scale, [7],

$$\sigma = \frac{P_t}{P_r}. \tag{3.6}$$

3.2.3 Rain Effect

In mmMwave communication, the rain loss is not negligible, [34]. The International Telecommunications Union Radio communication (ITU-R) section already has a model for corresponding signal attenuation for a given rain rate and operating frequency band, [35]. The model is built on a relatively low rain rate of between 15 mm/h and 20 mm/h, [34]. The signal attenuation due to rainfall is denoted as γ_R. The ITU-R power-law relationship model is expressed in Eq. (3.7)

$$\gamma_R = k * R^{\Gamma}. \tag{3.7}$$

Here, γ_R is the signal specific attenuation expressed in dB/km, while R is the given rain rate in mm/h. Then, k and Γ are polarization coefficients that are determined based on the operating frequency band. In ITU-R model, the supported frequency ranges from 1 GHz to 1000 GHz, [35]. Finally, in our work, the effect of foliage is assumed to be negligible in urban macro environments.

3.2.4 Fading Effect

Fading is due to variations in the wireless channel conditions. In our work, fading is modeled as a Rayleigh flat fading channel. Rayleigh distribution is zero-mean, with a unit-variance complex Gaussian distribution, $X \sim \mathcal{N}(\mu, \sigma^2)$, [7]. Rayleigh fading is modeled as

$$\phi(t) = X_I(t) + jX_Q(t). \tag{3.8}$$

Here, $\phi(t)$ is the channel realization at time (t) based on Gaussian distribution, X_{I} is the in-phase component of the channel realization, and X_{Q} is the quadrature component of the channel realization.

3.2.5 Total Channel Loss

The entire channel effect is taken as a summation of all the above listed signal loss components, in decibel. The total channel loss is expressed as

$$P_{\mathrm{loss}} = L + \sigma + \gamma_R + \phi. \tag{3.9}$$

Here, L, σ, γ_R and ϕ values are all in dB. The inverse of the channel loss value in the linear scale will give the channel gain.

3.3 Interference

In our work, signal interference is taken as the summation of every other received power at a reference point, MBS or SBS, apart from the dominant signal we are interested in. Interference is expressed as

$$I_{UEi} = \sum P_{\mathrm{EIRP}j} + G_{r_j} - L_j - \sigma_j - \gamma_{R_j} - \phi_j. \tag{3.10}$$

3.4 SINR and Baseline SINR Value

SINR refers to the capability of the channel to transmit information. SINR is usually used to estimate the quality of the received signal. SINR is the dominant received signal power divided by the sum of all other received signal power plus the noise in the channel. The SINR, P_r and interference, I are related as

$$SINR = \frac{P_r}{I + N_0}. \tag{3.11}$$

Here, N_0 is the modeled channel noise, which is a summation of the noise figure of the receiver, N_f, and the thermal noise, T_0. Then, I is the summation of all interference powers.
Given a baseline SINR value and the UE operating bandwidth, the achievable data rate of the channel is thus calculated as

$$R_b = BW * \log_2(1 + SINR). \tag{3.12}$$

Here, R_b is the achievable data rate in bits per second, and BW is the channel Bandwidth, in Hz. In other words, if given a target data rate and operating bandwidth, the minimum SINR, $SINR_{\text{min}}$, required per UE is determined by

$$SINR_{min} = 2^{\frac{R_b}{BW}} - 1. \tag{3.13}$$

Then the value is converted to decibel (dB) by the expression below:

$$SINR_{\text{dB}} = 10 * \log_{10}(SINR_{\text{min}}) \tag{3.14}$$

3.5 Receiver Sensitivity

Receiver sensitivity is the minimum received power that can be detected at the receiver for useful communication. In our work, the receiver is the BS and the receiver sensitivity must satisfy the minimum SINR value required per UE. Receiver sensitivity is therefore expressed as

$$RCV = SINR_{\text{min}} + N_0. \tag{3.15}$$

Here, SINR_{min} is the minimum SINR to guarantee the modeled minimum data rate per UE. All values are in dB.

3.6 Resource Block

5G NR offers a flexible channel bandwidth based on the SCS value selected. The bandwidth occupied by an RB depends on the SCS value in use. Our model assumes that one UE uses a minimum of one RB at a given time. The bandwidth capacity for one RB is determined by

$$BW_{\text{RB}} = 12 * SCS. \tag{3.16}$$

Here, BW_{RB} is the bandwidth occupied by one RB, and 12 represents the 12 consecutive sub-carriers in one RB. It also taken that there is always at least one RB available for each SBS at all times. The total number of RBs is determined by

$$RB_s = \frac{BW}{BW_{RB}}. \tag{3.17}$$

3.7 UE and SBS Association

The UE association is based on the CSI the UE receives from the MBS and SBS periodically. The SBS association is based on the CSI the SBS receives from the MBS periodically. The UE after receiving the CSI from all the BSs, will determine its channel quality to all the BSs, from its present location. After comparison, the UE will be associated with the BS, MBS or SBS, that offers the best channel quality at that time. Here, the best channel quality means the channel that offers the highest received signal power at the BS. Likewise, the SBS will associate with

the MBS that offers the best channel quality at a given time. The SBSs are all stationary. The association strategy for the UE is expressed as

$$A = \begin{cases} 1, & \text{if } P_{ri} \geq P_{r\mathrm{A}}, \forall\, A \in U, \\ 0, & \text{otherwise,} \end{cases} \tag{3.18}$$

where A is a number of UEs associated with a BS and U is a set of all the UEs within the service coverage area. Association can be to MBS or to SBS_j. On the other hand, the association strategy for the SBS is expressed as

$$W = \begin{cases} 1, & if P_{ri} \geq P_{r\mathrm{W}}, \forall\, W \in Z, \\ 0, & \text{otherwise,} \end{cases} \tag{3.19}$$

where W is the number of SBSs associated with the MBS and Z is a set of all the SBSs within the service coverage area.

3.8 Service Coverage Probability

For our work, service coverage probability (ρ) is defined as the ratio of the UEs within the target coverage area that can meet the minimum requirements of SINR value and data rate at a given instant, to the total number of UEs transmitting within the coverage area of the MBS. Also, ρ is expressed as a percentage. The major control metric for our simulations is ρ. Service coverage probability is expressed as

$$\rho = \frac{E_m}{E} \times 100. \tag{3.20}$$

Here, E_m is the number of UEs that meet the minimum requirements for the service and E is the total number of UEs randomly placed within the targeted service coverage area, using FHPPP.

3.9 Achievable Data Rate of the UE

The achievable data rate of a UE within the service coverage is the amount of data that UE can transmit to its associated BS. The same concept holds for any SBS associated with a MBS. It is modeled as

$$R_b = BW * \log_2(1 + SINR_i). \tag{3.21}$$

Here, $SINR_i$ is the SINR value at the receiver side of the BS for a given UE_i.

3.10 Access and Backhaul Bandwidth Utilization

Based on the allocated bandwidth, the maximum number of RBs that the wireless channel supports is 270. These RBs are shared between the access links and backhaul links depending on the instantaneous demand from the UEs and SBS. Then, the

access bandwidth is directly related to the number of UEs that are associated with the MBS or SBS at a given time, and the number of RBs per UE. Whereas, the backhaul bandwidth is directly related to the total number of RBs used in access link by the UEs plus the total number of RBs pre-allocated to the SBS. Since 1 RB translates to a finite bandwidth value, then the access bandwidth is expressed as

$$BW_{\text{Access}} = BW_{\text{RB}} * RBs * E_{\text{AccessUE}}. \tag{3.22}$$

With the channel bandwidth being shared between the access and backhaul links, the expression below holds

$$\begin{cases} BW_{\text{Access}}, & = \beta\, BW. \\ BW_{\text{Backhaul}}, & = (1-\beta)\, BW. \end{cases} \tag{3.23}$$

Here, E_{AccessUE} is the total number of UEs associated with the MBS and SBSs, BW_{Access} is the instant access bandwidth in use, and BW_{Backhaul} is the instant backhaul bandwidth in use. BW_{Access} and BW_{Backhaul} can then be weighed against the allocated channel bandwidth, BW. The percentage of the bandwidth resources used in the access links is represented as β, where $\beta \in [0,1]$.

3.11 TDD Scheduler for MBS/SBS/UE

Based on the assumption that all nodes are centrally synchronized and transmission from all nodes are scheduled, the following TDD scheduling epochs are considered as the transmission time for the MBS, SBS and UE within the network in uplink communication.

(i) When the SBS is transmitting, Fig. 3.3, the MBS and UE are receiving. Interference is only among the SBSs.

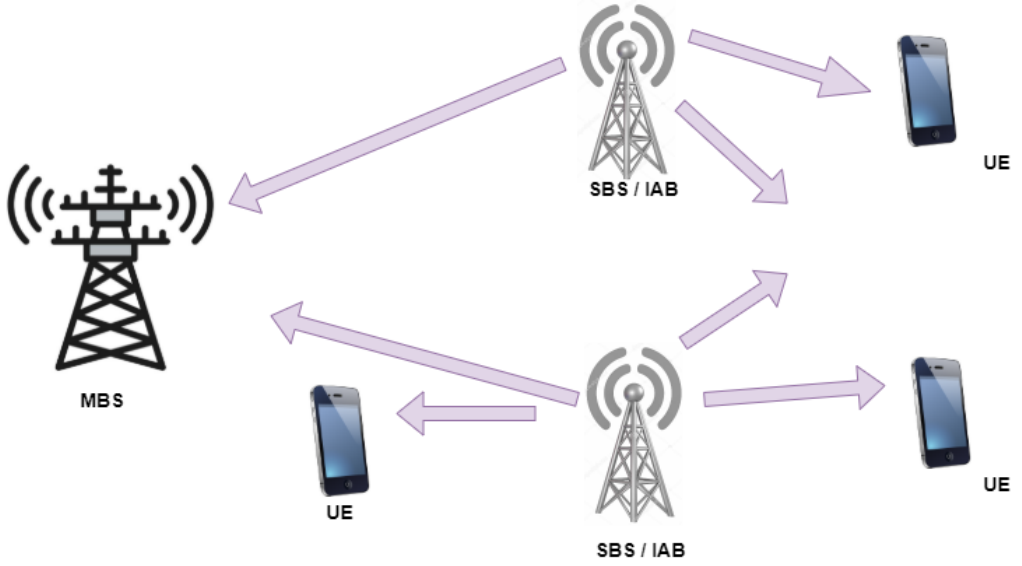

Figure 3.3: First TDD Epoch. Here, only SBSs are transmitting within the cell.

(ii) When the UE is transmitting, Fig. 3.4, the MBS and SBSs are receiving. Interference is only among the UEs inside the coverage area of the MBS.

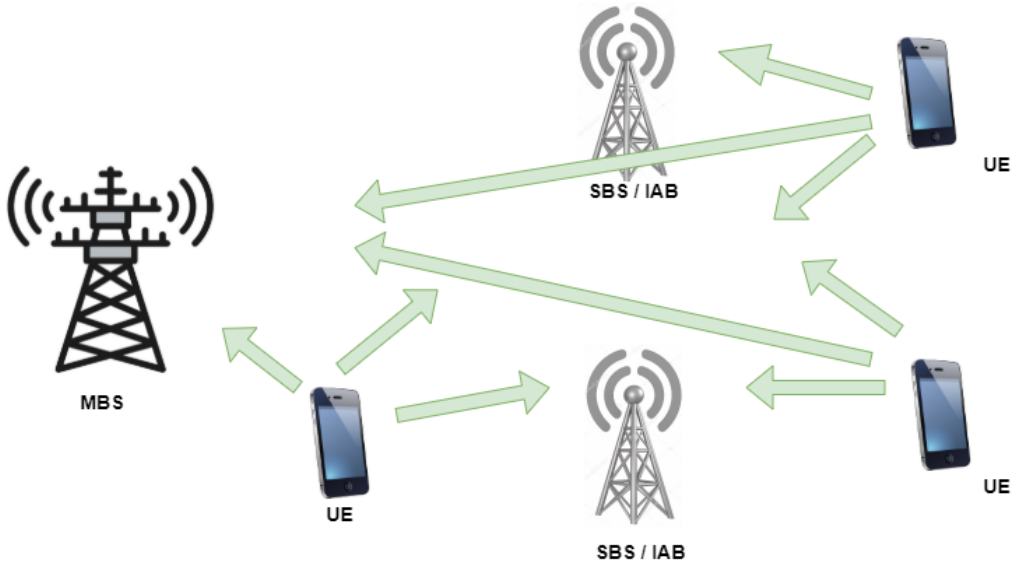

Figure 3.4: Second TDD Epoch. Here, only the UEs are transmitting within the cell.

(iii) Special case: when the SBS and UEs associated with the MBS only are transmitting, Fig. 3.5. Here, all other UEs and the MBS are receiving. The special case creates an opportunity to observe the effect of having the access and backhaul communication happening at the same time.

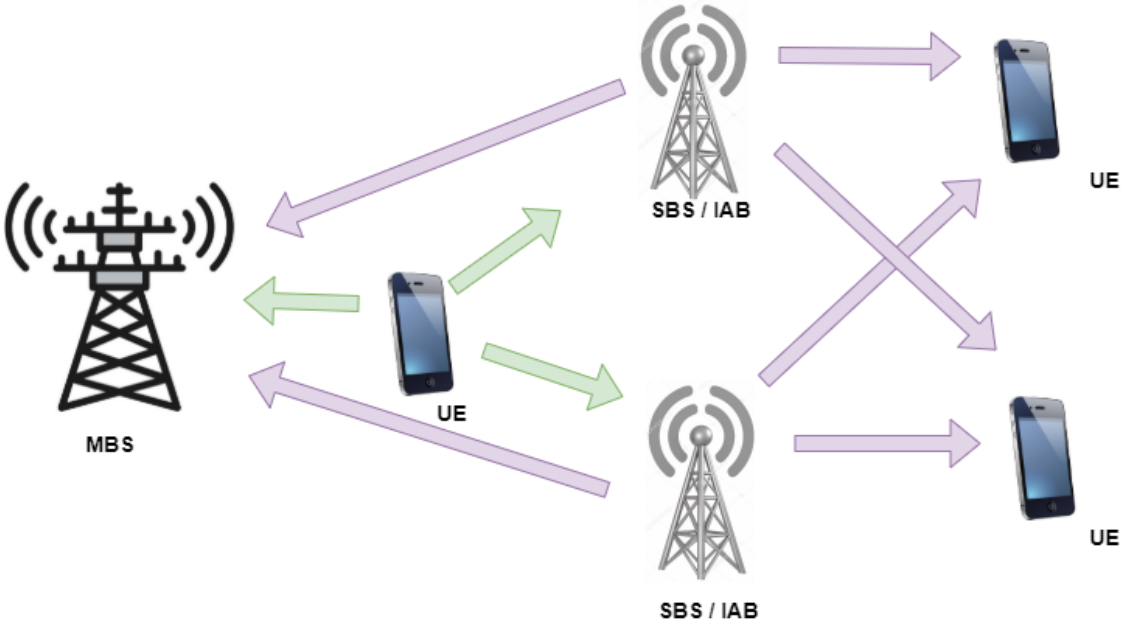

Figure 3.5: Special TDD case. Here, only the SBSs and the UEs associated with the MBS are transmitting.

3.12 Genetic Algorithm for Power Control

A baseline algorithm is needed for proper evaluation of the solutions to the formulated power control problem. Also, with a baseline algorithm the entire process is broken into clear steps, detailing possible aspects that may be refined and allowing logical inferences to be drawn from the results. For this reason, GA is selected as a baseline algorithm for a proper solution to the problem formulation, [39]- [42]. GA is independent of the channel realizations which means that the final solutions offered by the algorithm are comparatively fair. The GA transmit power control algorithm is formally expressed as

Algorithm 1 GA-Transmit Power Control Algorithm

For each instance in N, with a set of MT that require power control, do the following:

1: Create K, e.g., $K = 10$, sets of transmit powers, randomly selected from the range between the minimum and maximum transmit power allowed for the MT. Each element in the set corresponds to a MT.
2: For each set, calculate the received power, SINR and outage probability.
3: Find the set with the lowest outage probability and set it as the queen.
4: Create $S \ll K$, e.g., $S = 5$, sets of randomly selected transmit powers around the queen. Then, calculate the received power, SINR and outage probability for each set.
5: Find the set that has the lowest outage probability and update the queen.
6: Create a $V = K - S - 1$ sets of transmit powers, with each element in the set related to the allowed transmit power for the MT.
7: Calculate the received power, SINR and the outage probability of the V set.
8: Compare the set which has the lowest outage probability with the queen. Then choose the one with the lowest outage probability as the queen.
9: Then go to back to **Step 2** and continue for N iterations.
10: Finally, return the queen as the optimal power solution which has lowest outage probability after N iterations.

The proposed GA algorithm is thus explained:

A value, N, is set as the number of iterations for the algorithm. The value is decided by the designer as the maximum number of iterations supported by the algorithm. As an example, $N = 20$. The first step starts by the selection of K number of iterations randomly, as a part of N iterations. As an example, $K = 10$. Then, a set is created containing randomly selected transmit powers, with each value coming from the pre-defined range of transmit power values supported by the MT. There is a minimum and maximum transmitted power allowed by 3GPP, based on the power class of the UEs. Next, the received power of that MT at the BS is calculated, as well as its corresponding SINR, and outage probability. Outage probability is the probability of the event that the UEs cannot meet the baseline service requirements. The process is then repeated for K number of iterations. At the end of K iterations, a set of transmit powers that offers the minimum outage probability is selected for K. The newly selected set is set as queen, and is kept for the next step. The second

step begins with generating $S << K$ sets of transmit power values around the queen, by making few mutations on it, i.e., changing one or two elements inside the queen. Next, the received power, SINR, and outage probability for each set is calculated. After that, the set with the minimum outage probability is selected and the queen is updated with new values. Therefore, a new queen is created. Going forward, the third step repeats the first step, which now offers a new queen value. Then, there is a comparison between the new queen from third step and the queen from the second step, to see which of them has the lowest outage probability. Finally, the set with the lowest outage probability now becomes the queen. The algorithm repeats all the three steps along N and takes the set that offers the lowest outage probability as the output.

4

Simulation and Results

This chapter presents the results from all the simulations performed using the various models and the GA. The uplink power control problem is approached as a multi-objective optimization problem. Different scenarios, test cases and parameters are tested to observe the behaviour of the models and learn about IAB networks. Table 4.1 shows the system parameters used in all the MATLAB simulations for the IAB network, except otherwise explicitly defined.

Table 4.1: Simulation Parameters.

Parameter	**Value**	**Parameter**	**Value**
f_c	28 GHz	r	200 m
BW	400 MHz	σ	4 dB
SCS	120 kHz	α	4
Min. Number of RB	24	$h^{'}$	1 m
Max. Number of RB	270	d_0	1 m
T_0	-174 + (10*$\log_{10}(BW)$)	M	4 in each cell
N_f	5 dB	$R_{b\,\text{Minimum}}$	64 kbps
N_0	T_0 + N_f	UE EIRP	{23 - 43} dBm
h_{MBS}	25 m	SBS EIRP	{35 - 53} dBm
h_{SBS}	{21 - 24} m	G_r	25 dB
h_{UE}	1.5 m	R	{15 - 20} mm/h

The models are deployed for an urban macro environment. The rain effect for 28 GHz band, based on ITU-R model, for different rain rates according to Eq. (3.7) is shown in Fig. 4.1. The MBS service coverage is modeled as a hexagon with a radius of 200 m and with four stationary SBSs associated with the MBS. Eq. (3.9) gives the total channel loss for any given UE or SBS. The pathloss exponent value is 4, i.e., $\alpha = 4$, which portrays a dominant NLOS communication in UMa scenarios. The receiver gain of each BS, G_r, is 25 dB, [38]. From Eq. (3.17), $\text{RB}_\text{s} \approx 277$. Since TDD is in use, some RBs were considered to be used for synchronization and guard time to mitigate co-channel interference, [28]. In order to have round figure, 270 is set as the maximum number of RBs in the set-up. Based on the number of SBSs per MBS and the assumption that at least one RB is always available to the SBS, the maximum number of RBs for the access link is 131 while for the backhaul is 139. Therefore, β is approximately 48% at best. Table 4.2 puts the sharing of RBs into context. Our work simulates with a maximum of 4 RBs per UE in all

cases. The baseline parameters are based on data rate, SINR, cell radius, RBs per UE, and the concurrent number of UEs within the cell. The KPI of interest is the service coverage probability, ρ. The minimum data rate of 64 kbps is selected based on the 3GPP as the minimum data rate for any UE to pass the integrity test in 5G NR, [36]. Table 4.2 shows a relationship between the allocated RBs per UE, access-backhaul RB utilization and the number of guaranteed UEs at a time within the cell. Analysis from Table 4.2 forms a basis for the upper limit of the number of UEs simulated in this work.

Table 4.2: Empirical sharing of resource blocks.

RB per UE	Number of Access RBs	Number of Backhaul RBs	Total RBs	Supported Number of UEs
1	131	139	270	131
2	130	140	270	65
3	129	141	270	43
4	128	142	270	32
5	130	140	270	26
6	126	144	270	21
7	126	144	270	18
8	128	142	270	16

However, with increasing number of RBs per UE, the number of concurrent UEs in the cell reduces. The backhaul link resource block utilization is always more than the access link in this context. From Eq.(3.12) and Eq.(3.13), increasing the bandwidth per UE, decreases the SINR requirement with a possibility of having higher data rates.

4.1 Effect of Rain

Based on ITU-R model from Eq.(3.7), Fig.4.1 is created for varying rain rate values. It shows that with increasing rain rate comes higher signal degradation.

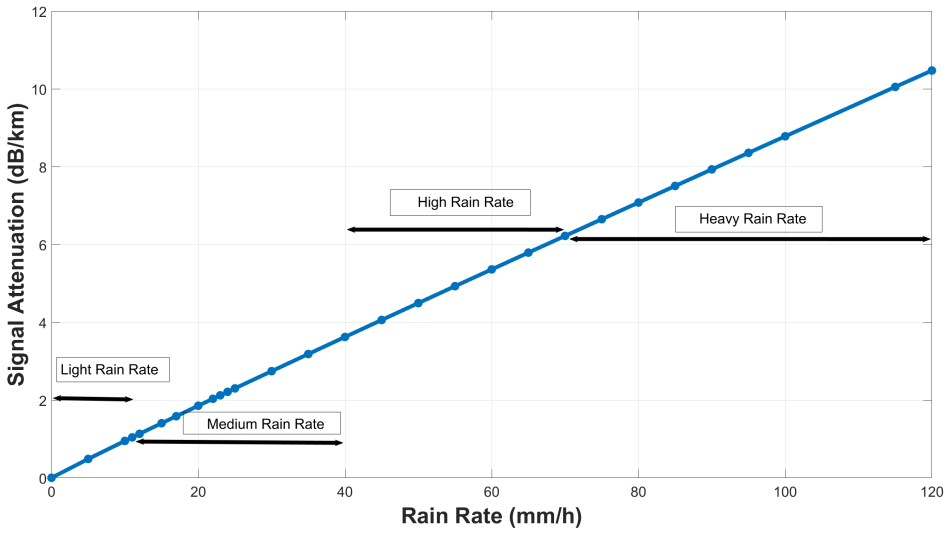

Figure 4.1: ITU-RP.838-3 rain loss for 28 GHz for varying rain rates up to 120 mm/h (r = 200 m, f_c = 28 GHz).

Notably, with a heavy rain rate, of 120 mm/h, the rain loss can reach 10 dB, which agrees with [37]. The rain loss is considerably high for mmWave communication that inherently has short wavelengths and is highly affected by blockage. The effect of rain on the service coverage probability is therefore not negligible. The model in this thesis considers rain rates between 15 mm/h and 20 mm/h.

4.2 Effect of Increase in RB per UE and Power Control (One Cell)

Here, we simulate a single cell, with a fixed cell radius, varying baseline data rates, and RBs per UE. The simulation starts with all UEs transmitting at a minimum power of 23 dBm, irrespective of their location in the cell and the wireless channel conditions. There is no power control at this stage. Afterwards, GA is introduced as a centralized controller that takes inputs about the channel conditions and the baseline service requirements to implement power allocation for all the UEs and SBSs. The simulation is broken into four test cases. The main investigation is to observe whether there is a correlation between the service coverage probability and the operating bandwidth per UE. The tests for 512 kbps to 5 Mbps are based on suggestions from GSMA, [20]. Figure 4.2 is an illustration of a single-cell IAB network.

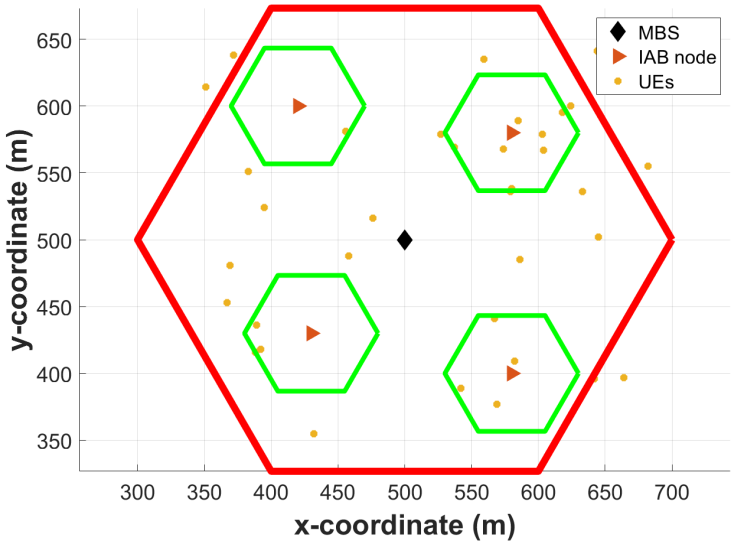

Figure 4.2: 2D illustration of 1 MBS single-cell with MATLAB.

Building on the premise of a TDD system, we investigate the service coverage probability with a separation of access and backhaul links in the time domain. With the considered two-hop network, the model follows that when the SBS (IAB node) is transmitting, the MBS and UEs are only receiving, Fig. 3.3. On the other hand, when the UEs are transmitting, the SBSs and MBS are receiving, Fig. 3.4.

The set-up is a single cell composed of one MBS and four SBSs. All BSs are stationary. The RB per UE is set as one and then increased in a step-wise manner to four RBs per UE. The cell radius is fixed at 200 m. The UEs are randomly distributed in the coverage area using FHPPP. The baseline data rate per UE is set as 64 kbps, and then increased to 512 kbps, 1 Mbps, 3 Mbps and 5 Mbps for the different test cases. Figures 4.3-4.6 shows the result from using 1 to 4 RBs per UE respectively.

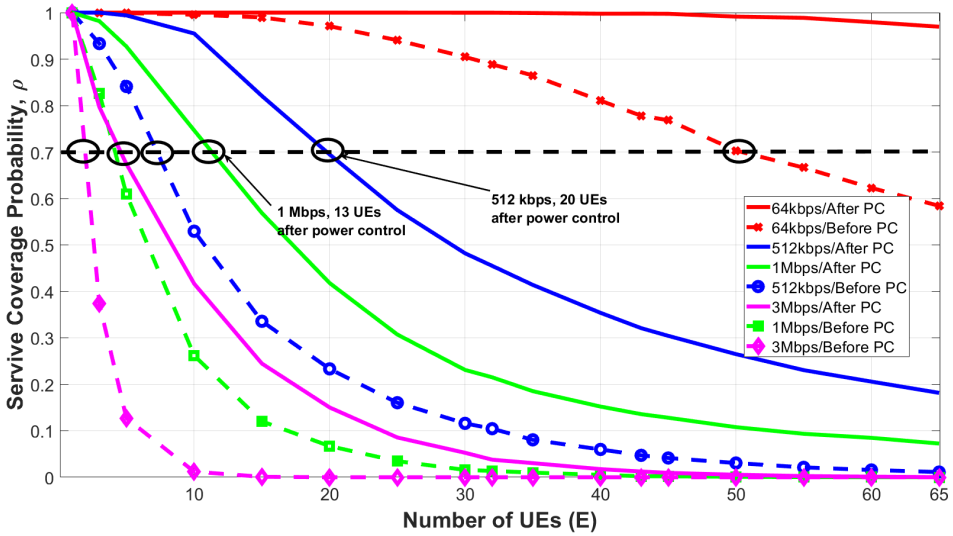

Figure 4.3: One cell: Service coverage probability versus the number of UEs with 1 RB per UE ($r = 200$ m, $M = 4$, $E = 65$).

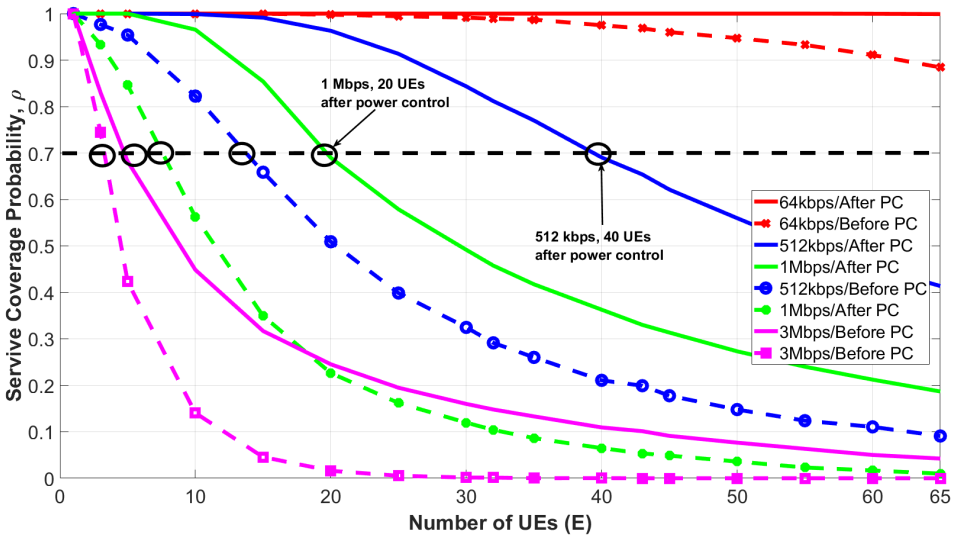

Figure 4.4: One cell: Service coverage probability versus the number of UEs with 2 RBs per UE ($r = 200$ m, $M = 4$, $E = 65$).

From all figures, it is observed that there is a downward trend in service coverage probability as the number of UEs associated with the BSs is increasing. Figure 4.3 shows that with increasing baseline data rate per UE, the decline in the service coverage probability follows the same trend. Interestingly, after power control, by using the GA, the service coverage probability improves in each test case. Moreover, taking a minimum of 70% service coverage probability in each test case, it is observed that all UEs pass the minimum integrity test after power control with 64 kbps baseline data rate. Furthermore, with increasing data rate requirement per UE, which directly results in increase in the minimum SINR requirement per UE, the service coverage probability starts to reduce. In abstraction, by setting the guaranteed data rate to be 1 Mbps at 70% service coverage probability, after power control, the achieved concurrent UEs is 18% while before power control the achieved concurrent UEs is 9%.

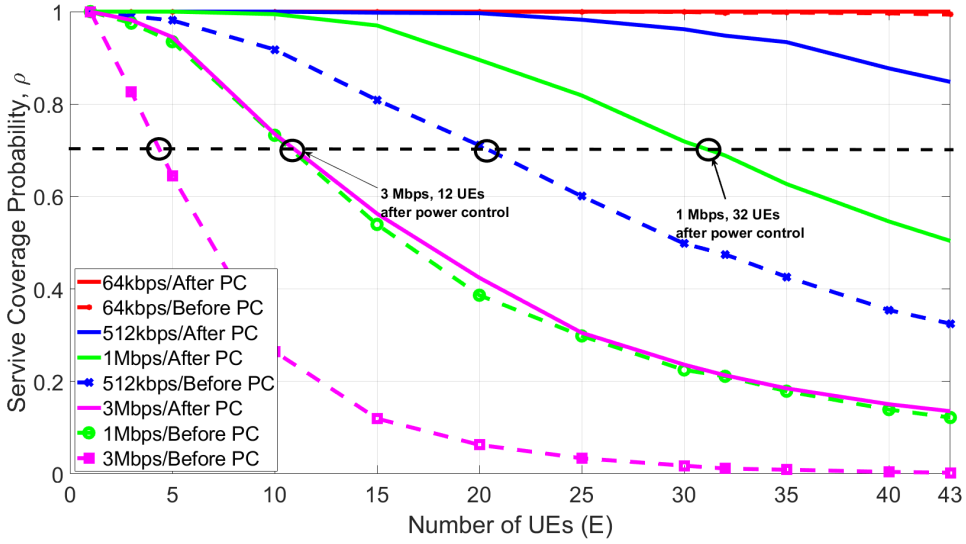

Figure 4.5: One cell: Service coverage probability versus the number of UEs with 3 RBs per UE ($r = 200$ m, $M = 4$, $E = 43$).

Furthermore, Figs. 4.4-4.6 are results from 3 other cases where the RB per UE is set as 2, 3 and 4 respectively. Moreover, based on Table 4.2, it is evident that as the number of RB per UE increases, the number of guaranteed concurrent UEs decreases. The results show that with 1 Mbps baseline data rate at 70% service coverage probability, after power control, the achievable concurrent UEs that meets the service requirements is 30% with 2 RBs per UE while before power control, the achieved concurrent UEs is 15% with 2 RB per UE. Meanwhile, with 1 Mbps baseline data rate at 70% service coverage probability, after power control, the achievable concurrent UEs that meets the service requirements is 74% with 3 RBs per UE versus 33% without power control. Furthermore, for the same constraints, the achievable concurrent UEs that meets the service requirements after power control is 100% with 4 RBs per UE compared to 43% for the cases without power control.

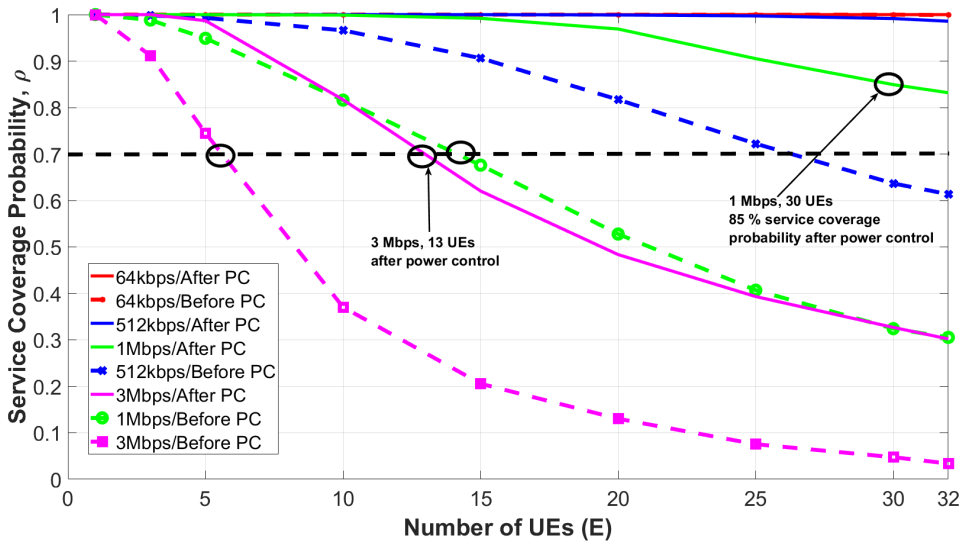

Figure 4.6: One cell: Service coverage probability versus the number of UEs with 4 RBs per UE ($r = 200$ m, $M = 4$, $E = 32$).

4.3 Effect of Increase in RB per UE and Power Control (Two Cells)

Here, our study is based on adjacent cell cases. We build on the assumption that there is a central synchronization and resource scheduling daemon, that enforces all BSs to transmit and receive at the same time, with the same TDD profile, in all cells. Each cell set-up is the same as in Section 4.2. Figure 4.7 is an illustration of our two adjacent cells set-up.

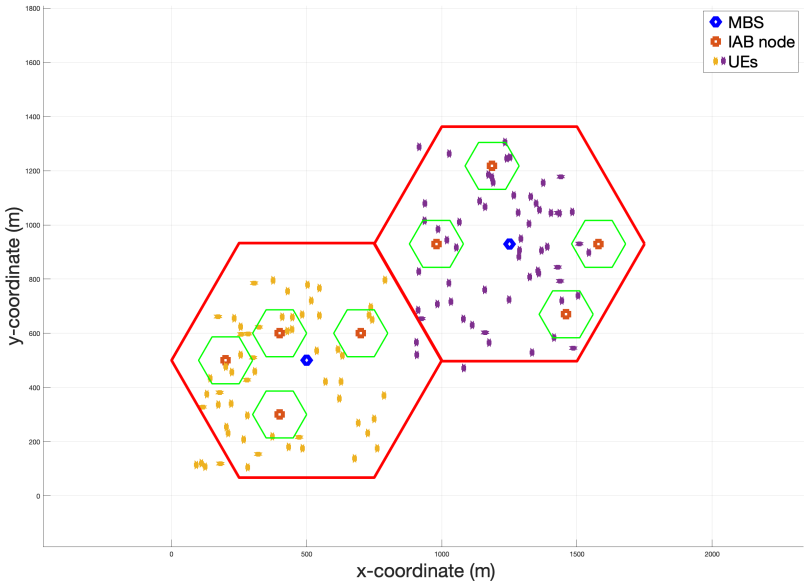

Figure 4.7: 2D illustration of 2 MBS adjacent cells with MATLAB.

Similar to Section 4.2, the UEs are randomly distributed within the service coverage area. The baseline data rate per UE is set as 64 kbps and increased to 512 kbps, 1 Mbps, and 3 Mbps for different test cases. Figure 4.8 shows the result with one RB per UE, and Fig. 4.9 shows the result with two RBs per UE. Also, Fig. 4.10 shows the result with three RBs per UE, and Fig. 4.11 shows the result with four RBs per UE.

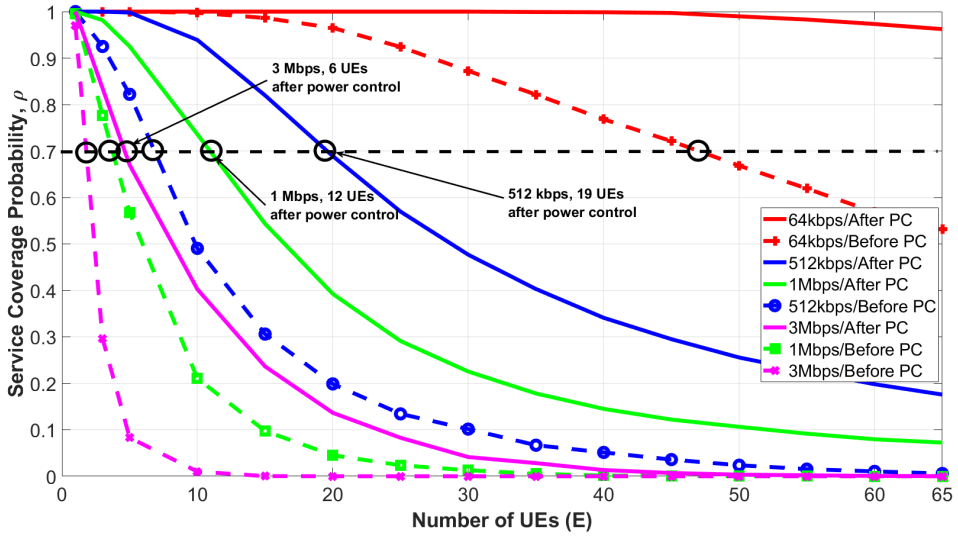

Figure 4.8: Two cell: Service coverage probability versus the number of UEs with 1 RB per UE ($r = 200$ m, $M = 4$, $E = 65$).

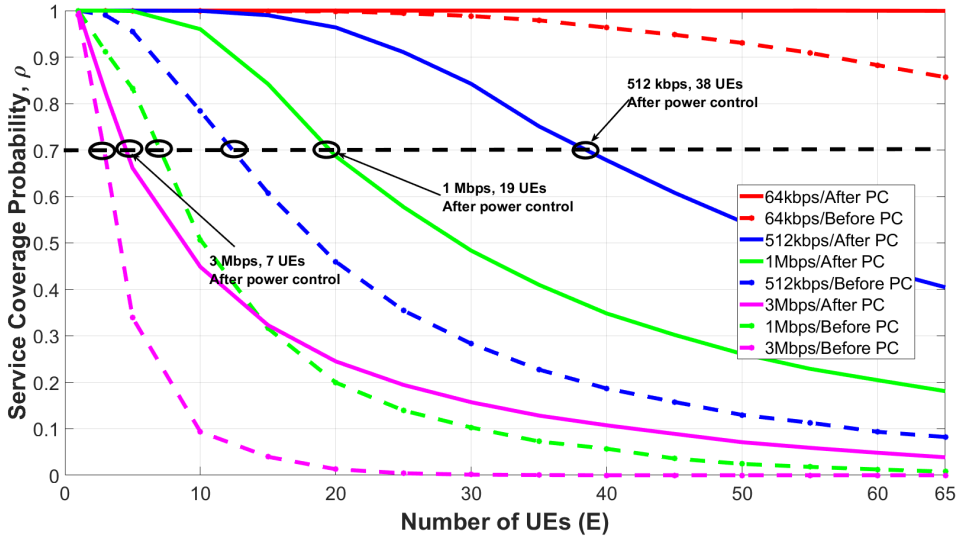

Figure 4.9: Two cell: Service coverage probability versus the number of UEs with 2 RBs per UE ($r = 200$ m, $M = 4$, $E = 65$).

From all figures, it is observed that there is a decline in the service coverage probability as the number of UEs per cell is increasing. Also, the same trend is observed as the data rate requirement per UE is increasing, the number of UEs that meets the minimum service requirement reduces. Comparing Fig. 4.8 with Fig. 4.9, it is seen that with 2 RBs per UE, the number of satisfied UEs at data rate of 512 kbps with 70% service coverage probability, after power control, increases by 100%. The improvement in service coverage probability may be attributed to a decrease in the SINR requirement as the operating bandwidth, or RB per UE, increases.

Figure 4.10 and Fig. 4.11 show the results from the cases with 3 RBs per UE and 4 RBs per UE in the two-cell set-up.

Notably, it is observed that the effect of inter-cell interference is minimal. The results show similarities with one cell test cases, Figs. 4.3-4.6. The observation may be attributed to the fact that a typical 28 GHz signal power is comparatively low and that the entire set-up is power-limited. Low inter-cell interference may encourage adjacent cells to have some overlap in service coverage area, thereby supporting seamless handover of UEs from one cell to another, without much increase in inter-cell interference.

Generally, from Sections 4.2 and 4.3, it is seen that with an increase in the RBs per UE, which also means an increase in the operating bandwidth of the UEs, the service coverage probability improves. The improvement is connected to the fact that with increasing bandwidth comes a reduced SINR requirement. The reduced SINR requirement results in reduced transmit power for all concurrent UEs and further reduces the interference within the cell. Also, the results point to the fact that power control offers increased service coverage probability in all cases.

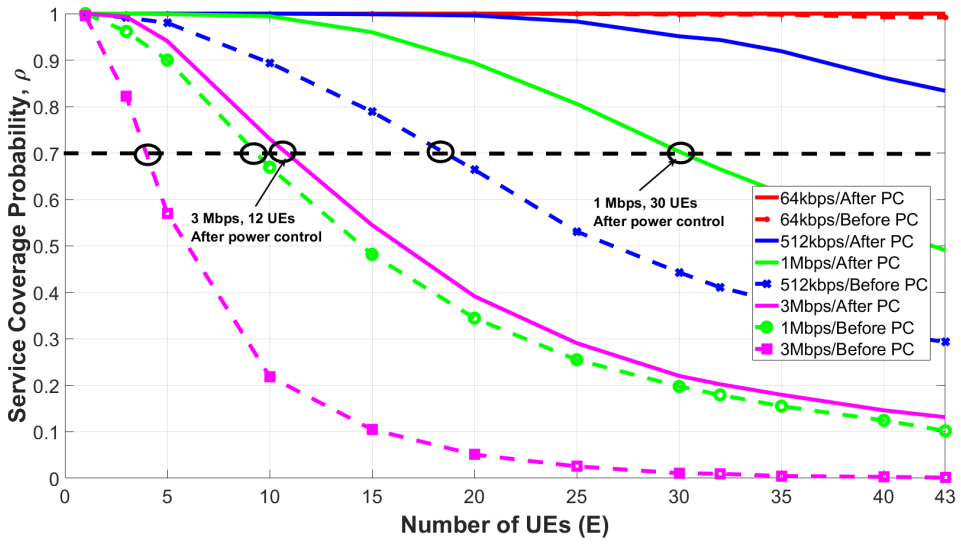

Figure 4.10: Two cell: Service coverage probability versus the number of UEs with 3 RBs per UE ($r = 200$ m, $M = 4$, $E = 43$).

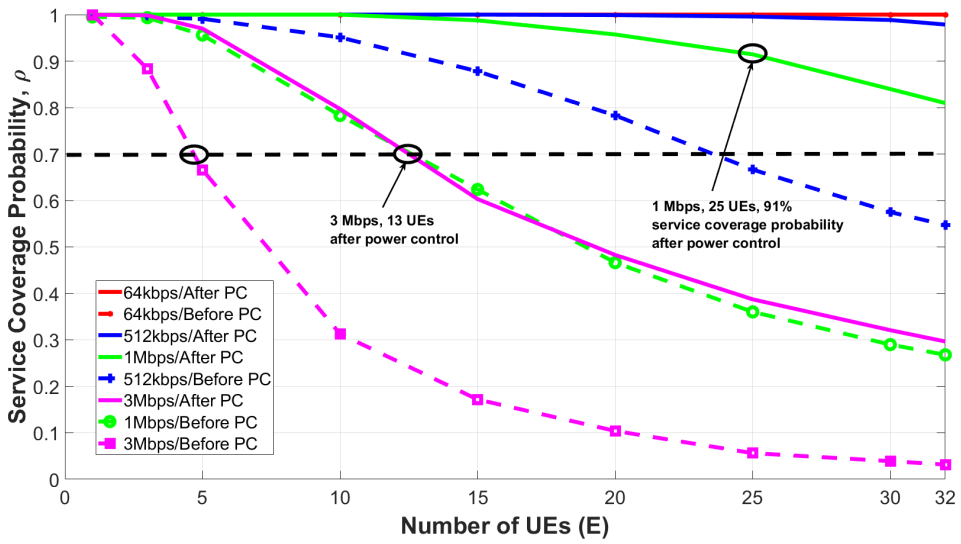

Figure 4.11: Two cell: Service coverage probability versus the number of UEs with 4 RBs per UE ($r = 200$ m, $M = 4$, $E = 32$).

Subsequently, the GA-based power control solution is built to guarantee an increase in service coverage probability. Power control with GA offers an increase in network capacity as the number of satisfied UEs increases. Although, the model is based on a constrained cell environment, it is assumed that there may be variations in service coverage probability as the cell size increases. Then, the edge UEs have to transmit with a higher power because the pathloss component of the channel loss increases with distance.

4.4 Effect of Interference on Simultaneous Access and Backhaul Links (One Cell)

During this test, the set-up is a single-cell IAB network, where the access and backhaul links are operating simultaneously. Here, the SBSs and the UEs associated with the MBS are the only entities transmitting at the same time. Similar to previous test cases in Section 4.2, there are 4 stationary SBSs and 1 MBS. The UEs are randomly distributed at each time, to simulate mobility. Figs 4.12-4.15, show the results from the test cases.

Similar to the other test cases in Section 4.2, there is an increase in service coverage probability as the number of RBs per UE is increases. The total number of empirically guaranteed UEs is still the same as portrayed in Table 4.2. Evidently, power control has a huge contribution to the overall performance of the cell set-up, as seen by comparing the service coverage probability before and after power control across all tested baseline data rates. Once again, 70% service coverage probability is used as the benchmark for comparison.

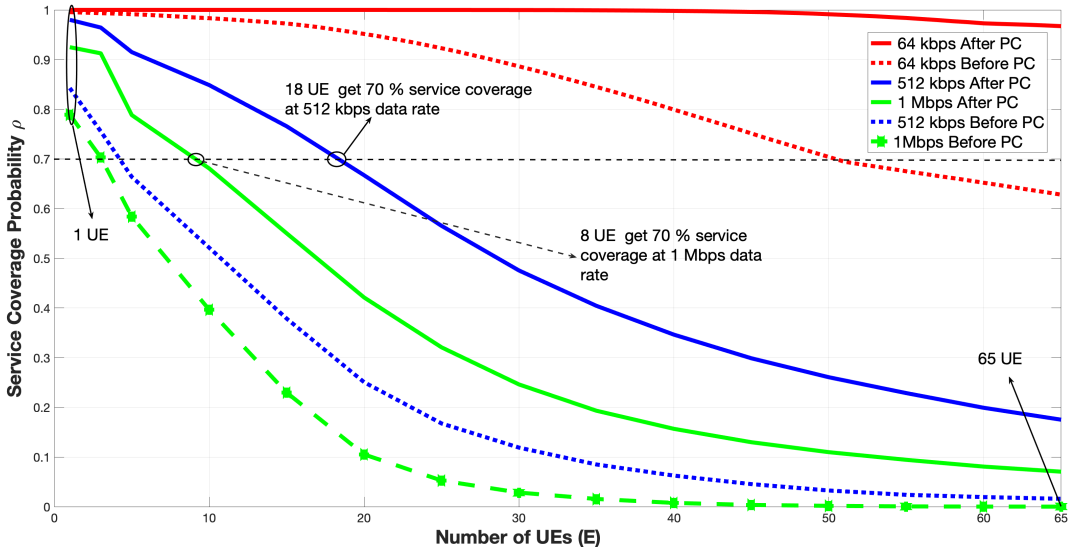

Figure 4.12: One cell: Service coverage Probability versus the number of UEs, with 1 RB per UE. The maximum number of UEs is 65, with 131 RBs for the access and 139 RBs for the backhaul.

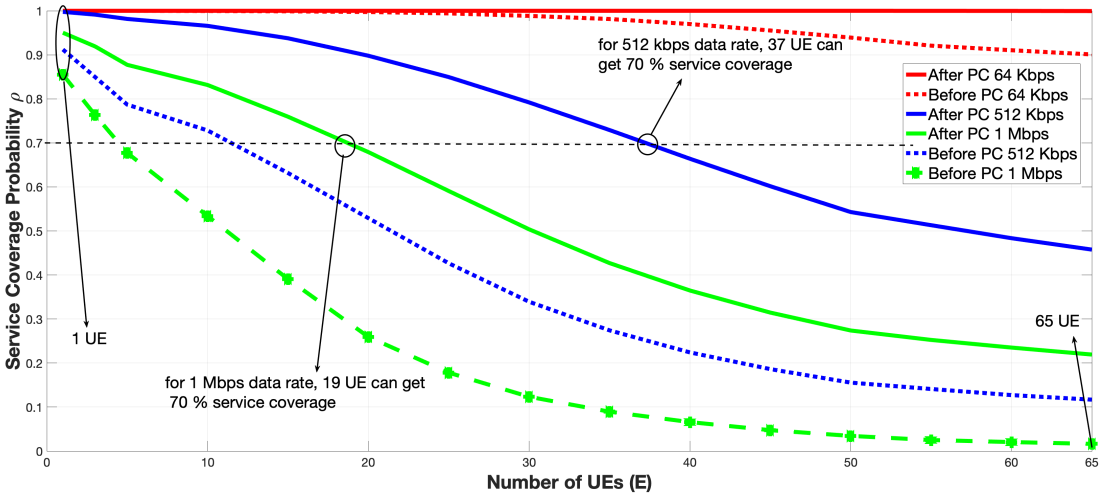

Figure 4.13: One cell: Service coverage Probability versus number of UEs, with 2 RBs per UE. The maximum number of UEs is 65, with 131 RBs for the access and 139 RBs for the backhaul.

By comparing Figs. 4.12-4.15, with the figures from Section 4.2, Figs. 4.3-4.6, it is seen that there is a decrease in the number of satisfied UEs within the cell. Figure 4.3 shows with 1 Mbps data rate, at 70% service coverage probability, after power control, the achieved concurrent UEs is 18%. Whereas Fig. 4.12 shows that with the same bench-marking parameters, only 13% of UEs satisfies the service requirements.

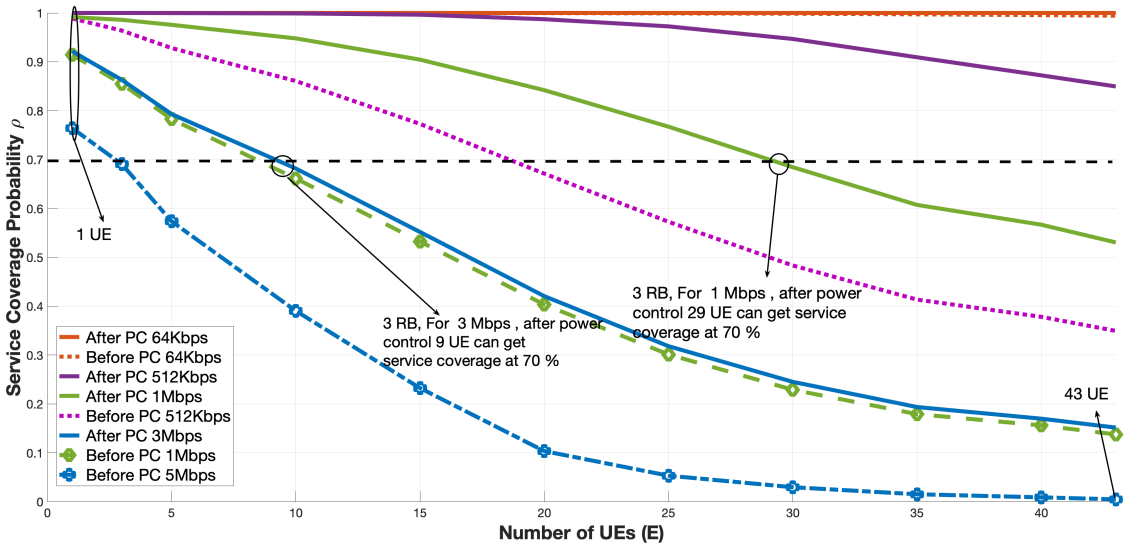

Figure 4.14: One cell: Service coverage Probability versus the number of UEs, with 3 RBs per UE. The maximum number of UEs is 43, with 131 RBs for the access and 139 RBs for the backhaul.

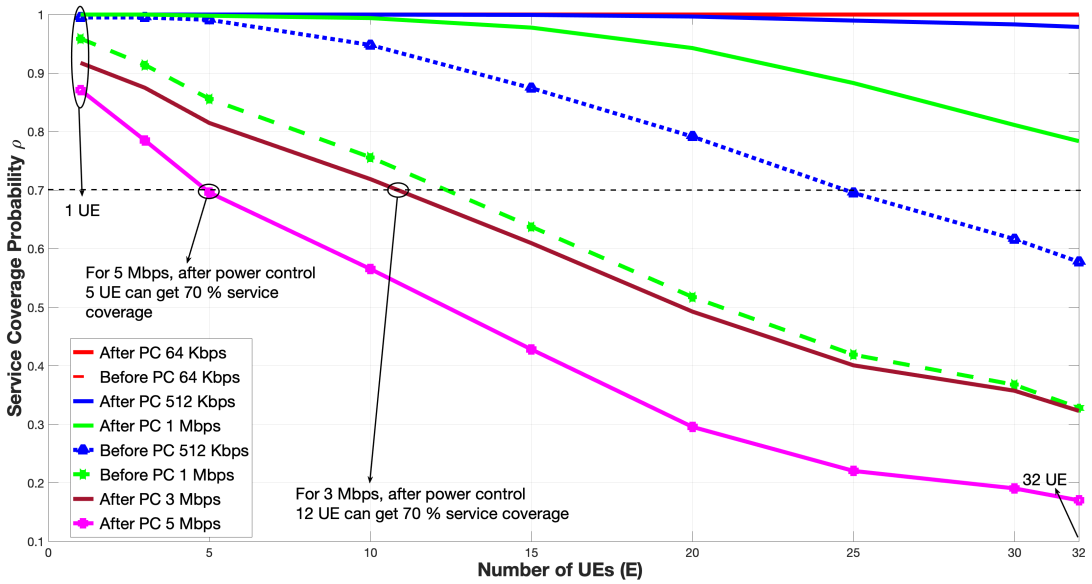

Figure 4.15: One cell: Service coverage Probability versus the number of UEs, with 4 RBs per UE. The maximum number of UEs is 32, with 131 RBs for the access and 139 RBs for the backhaul.

Evidently, an increase in the number of concurrent UEs transmitting within a cell leads to a gradual decrease in the service coverage probability. For instance, comparing Fig. 4.4 with Fig. 4.13, it is seen that in Fig. 4.4 with 512 kbps baseline data rate, at 70% service coverage after power control, the achievable concurrent UEs is 60%, while in Fig. 4.13, with 512 kbps baseline data rate, at 70% service coverage

after power control, the achievable concurrent UEs is 57%. Also, Fig. 4.5 shows that with 3 Mbps baseline rate, at 70% service coverage after power control, the achievable concurrent UEs is 28%, while in Fig. 4.14, with the same baseline, shows 20% of UEs can satisfy the service requirement at 70% service coverage probability. The observation may be attributed to the fact that the interference power that each UE_i has to contend with is increasing, as well as the interference between the access and backhaul links in TDD.

Moreover, the advantage of separating the access and backhaul links in TDD is seen in all test cases as the service coverage probability, before and after power control, is higher in Section 4.2 than when they operate simultaneously in this test case. Although, with 64 kbps as the minimum data rate, there seem to be no difference. The unnoticeable difference may be attributed to a low data rate and SINR requirement which is needed for UE control or signaling within the IAB network. Generally, in TDD profile, there are RBs used for synchronization between the transmitter and the receiver, [7]. The synchronization creates guard time between the UL and DL thereby guaranteeing a stable communication system and reducing interference. Without proper synchronization, simultaneous transmission in TDD reduces the signal quality. The results from these test cases points to this fact, that overlap in RBs due to simultaneous UL and DL reduces the service coverage probability.

4.5 Effect of Interference on Simultaneous Access and Backhaul Links (Two Cells)

The set-up during this test consists of two adjacent MBS cells where the access and backhaul links are operating simultaneously. The SBSs and the UEs associated with the MBS are the only entities transmitting at the same time.

Interference occurs between the UEs associated with the MBS and all the SBSs. The number of UEs associated with the MBS is a fraction of the total number of UEs randomly placed in the cell. There is a possibility of the UEs transmitting more power to overcome the interference from the SBSs, whose minimum transmit power is 35 dBm. Also, this set-up investigates the effect of inter-cell interference on service coverage probability with simultaneous operation of the access and backhaul links. The results of the test cases are shown in Figs. 4.16-4.19.

In all cases, the cell radius in each cell is fixed. The varying parameters are the data rates, number of concurrent UEs and the RBs per UE. The set-up cell coverage is modeled as a hexagon avoiding overlap from the other cell. The random distribution of the UEs provides the possibility of having UEs located at the edge of the cells, thereby contributing to inter-cell interference.

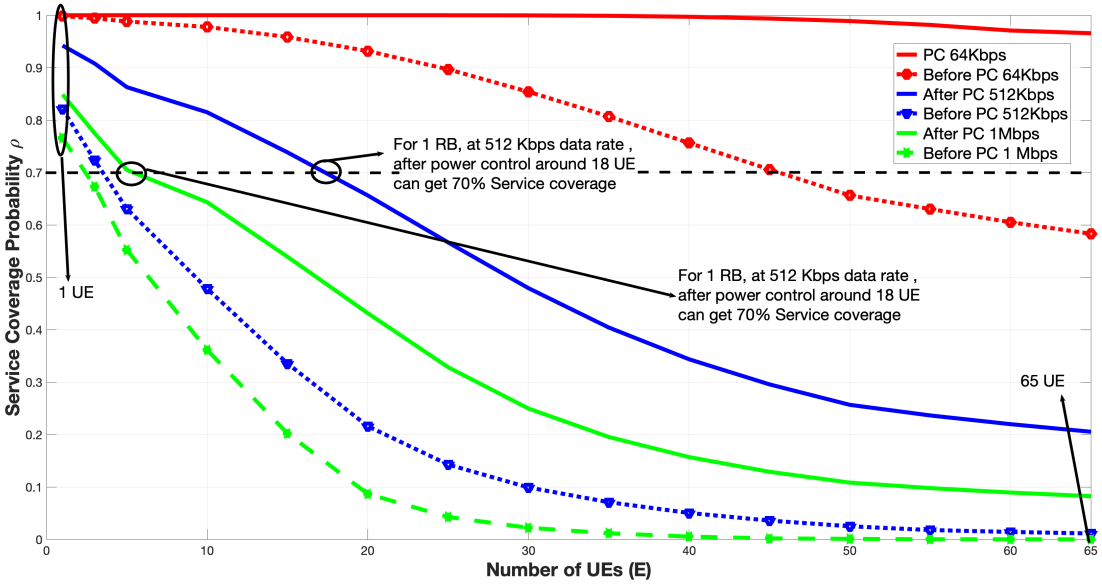

Figure 4.16: Two cell: Service coverage probability versus the number of UEs, with 1 RB per UE. The maximum number of UEs is 65, with 131 RBs for the access and 139 RBs for the backhaul.

Here, it is observed that the number of satisfied UEs is at the lowest compared with other scenarios and test cases. The observation may be due to increase in the interference power that the UEs are contending with. The set-up has both intra-cell and inter-cell interference at the same time. The combined interference may explain why the results here offer the lowest service coverage probability when compared with other simulations.

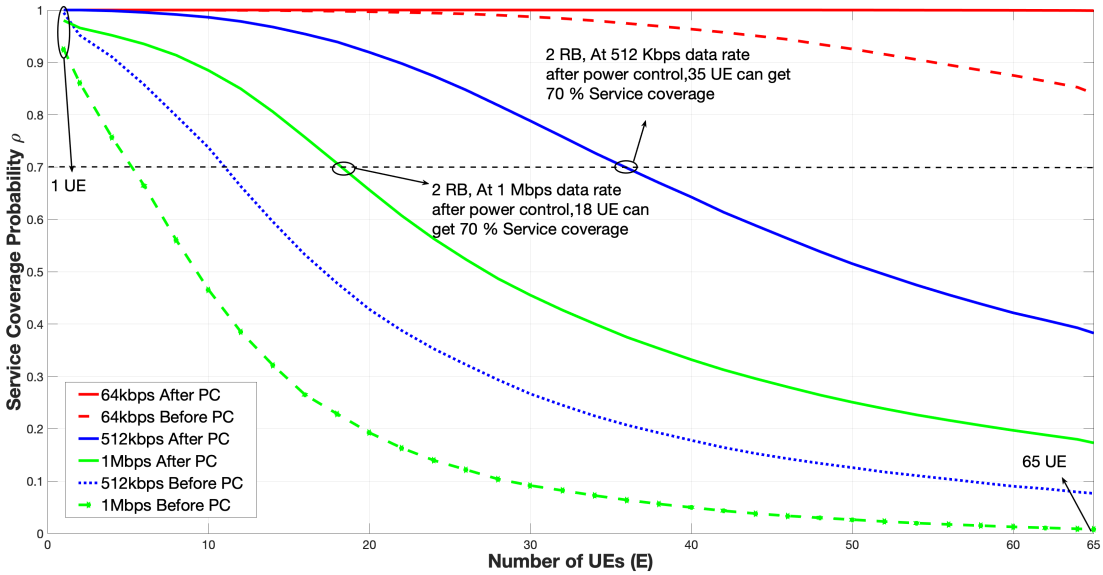

Figure 4.17: Two cell: Service coverage probability versus the number of UEs, with 2 RBs per UE. The maximum number of UEs is 65.

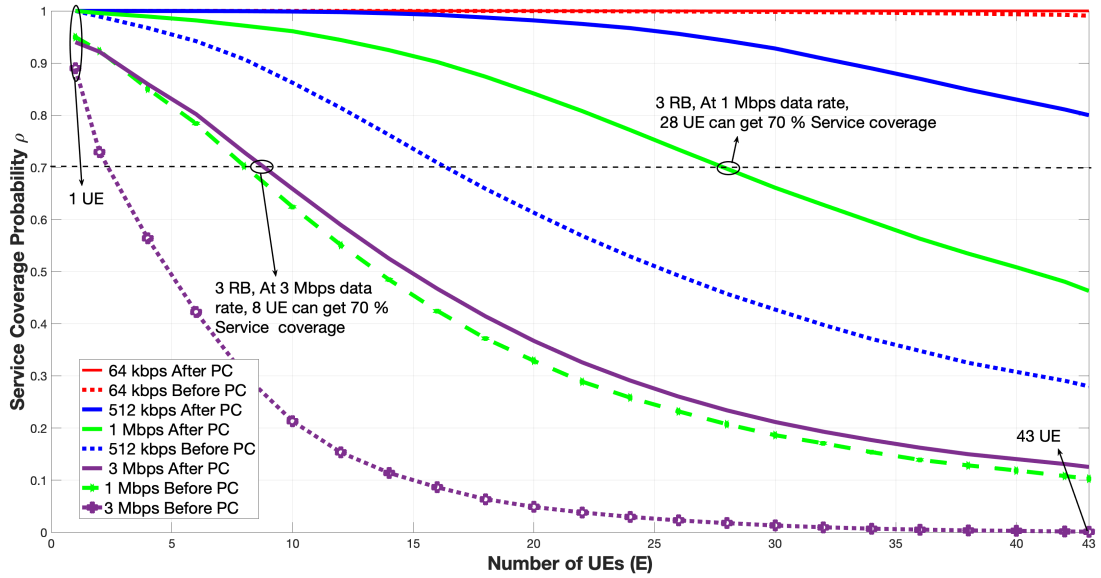

Figure 4.18: Two cell: Service coverage probability versus the number of UEs, with 3 RBs per UE. The maximum number of UEs is 43.

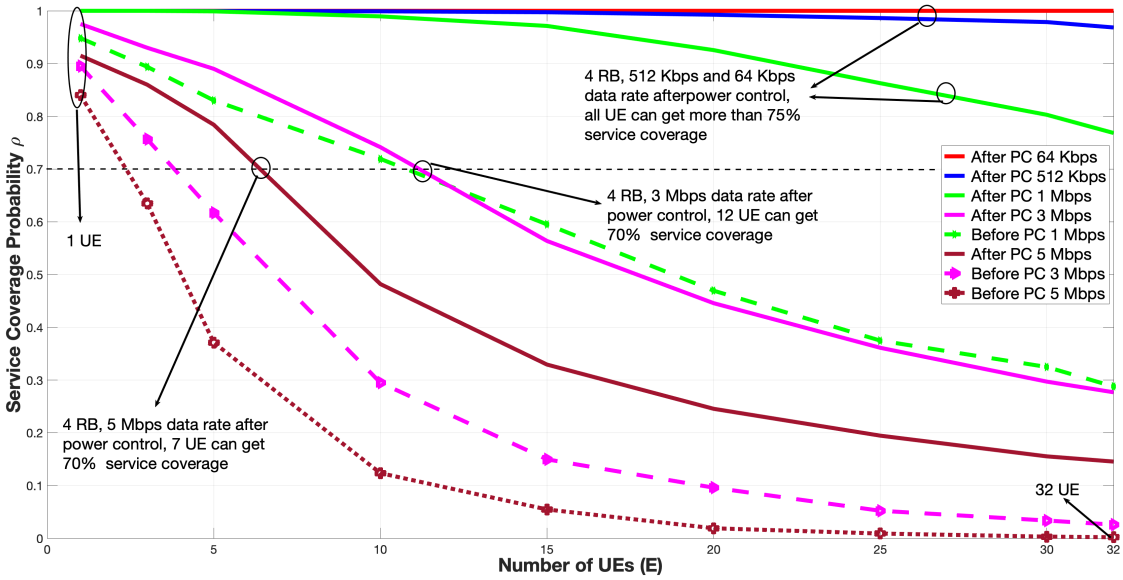

Figure 4.19: Two cell: Service coverage probability versus the number of UEs, with 4 RBs per UE. The maximum number of UEs is 32.

By comparing Fig. 4.16 with Fig. 4.8, it is seen that with 1 Mbps baseline data rate, and at 70% service coverage after power control, the achievable UEs that can satisfy the service requirements is 10% in Fig. 4.16, while the achievable UEs is 18% in Fig. 4.8, under the same constraints. With 2 RBs per UE, Fig. 4.17 shows that 57% of UEs satisfies the service requirements after power control. Furthermore, in Fig. 4.9, there are 60% of the concurrent UEs meets the same service requirements

after power control. Then, Fig. 4.11 shows that 40% of the concurrent UEs with 3 Mbps baseline data rate, meets the service requirements at 70% service coverage probability after power control, versus in Fig. 4.19, which shows that 36% of the concurrent UEs meets the service requirements at 70% service coverage probability after power control.

Here, the increase in the interference power affects the access and backhaul links working at the same time. Without proper separation between the RBs used in the access and backhaul links, the service quality may reduce. The decrease in service quality reflects in the number of UEs actively within the cell and the decrease in service coverage probability. Also, having high performing backhaul links is important for the RAN. If the performance of the backhaul links is low, it reflects in the performance of the access links as well.

4.6 Data Rate Analysis for the UEs

Based on the Eq. (3.21), the achievable data rates per UE is being observed. Building on the results from Sections 4.2 and 4.4, Figs. 4.20-4.23 are generated. The figures compares the actual UE data rates after power control versus the service coverage probability. The analysis is done for cases with 1 RB per UE and 4 RBs per UE. The investigation is looking at the average guaranteed data rate per UE, with and without power control, given a number of concurrent UEs within the set-up.

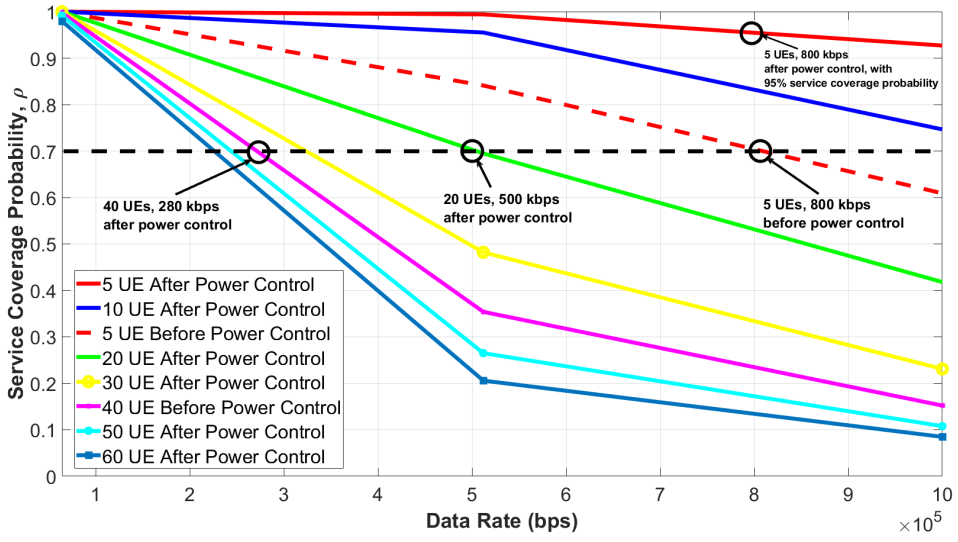

Figure 4.20: One cell: Service coverage probability versus the data rate with 1 RB per UE, $R_b = 1$ Mbps. The analysis is for the data rate values after power control.

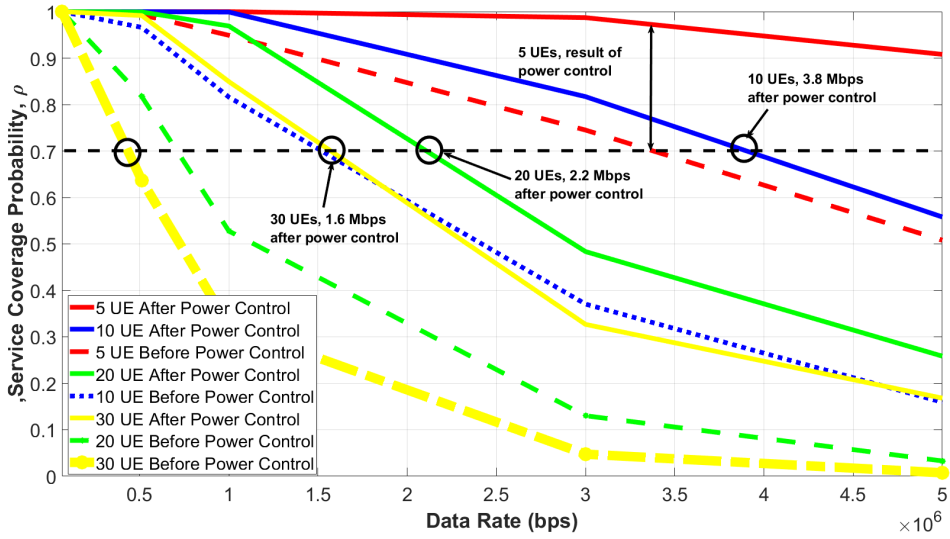

Figure 4.21: One cell: Service coverage probability versus the data rate with 4 RBs per UE, $R_b = 5$ Mbps. The analysis is for the data rate values after power control.

Figure 4.20 shows that with 1 RB per UE with 5 UEs, the service coverage probability varies between 100% to 60%, before power control, as the number of UEs are increasing. Furthermore, as power control is introduced, the service coverage probability started at 100% in all cases and then started declining as the number of concurrent UEs are increasing.

However, the service coverage probability increases after power control compared with the cases without power control. For example, with 5 UEs without power control at 70% service coverage probability, the achievable data rate is 350 kbps while after power control, 5 UEs get minimum service coverage at 93%, the achievable data rate is 1 Mbps. As seen in Fig. 4.21, with 4 RBs per UE, all service coverage probability values started from 100% both before and after power control. The same trend of decline in service coverage probability is seen as compared to Fig. 4.20. Also, there is the improvement in service coverage probability after power control compared with before power control, and the achievable data rate is higher since the operating bandwidth per UE increases. The increments in data rates after power control is 100% in all the number of UEs tested in both models (1 RB per UE and 4 RBs per UE).

Notably, in Fig. 4.20, with 20 UEs at 70% coverage probability, the achievable data rate is 512 kbps. Whereas, in Fig. 4.21, a The result shows that by increasing the number of RBs per UE, under the same constraints, the achievable data rates per UE increases. Increase in the number of RBs per UE offers better service coverage probability, lowers the SINR requirement and increases the achievable data rates. Conversely, as earlier stated, increase in RBs per UE comes at a cost of reduced number of UEs that the cell can support at an instant, since the allocated channel

bandwidth is fixed.

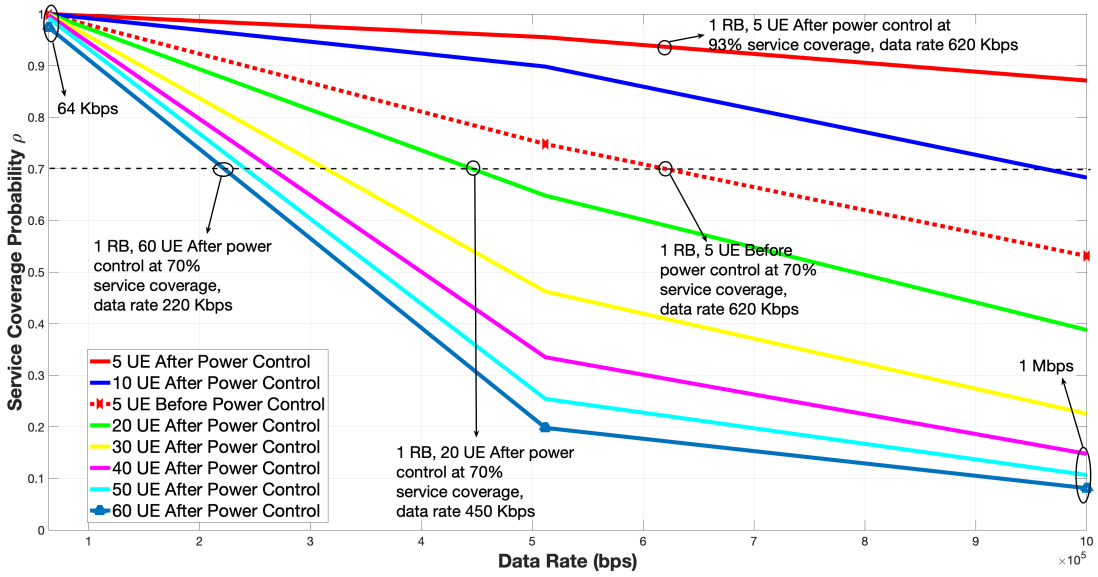

Figure 4.22: One cell special case: Service coverage probability versus the data rate with 1 RB per UE, $R_b = 1$ Mbps. The analysis is for the data rate values after power control.

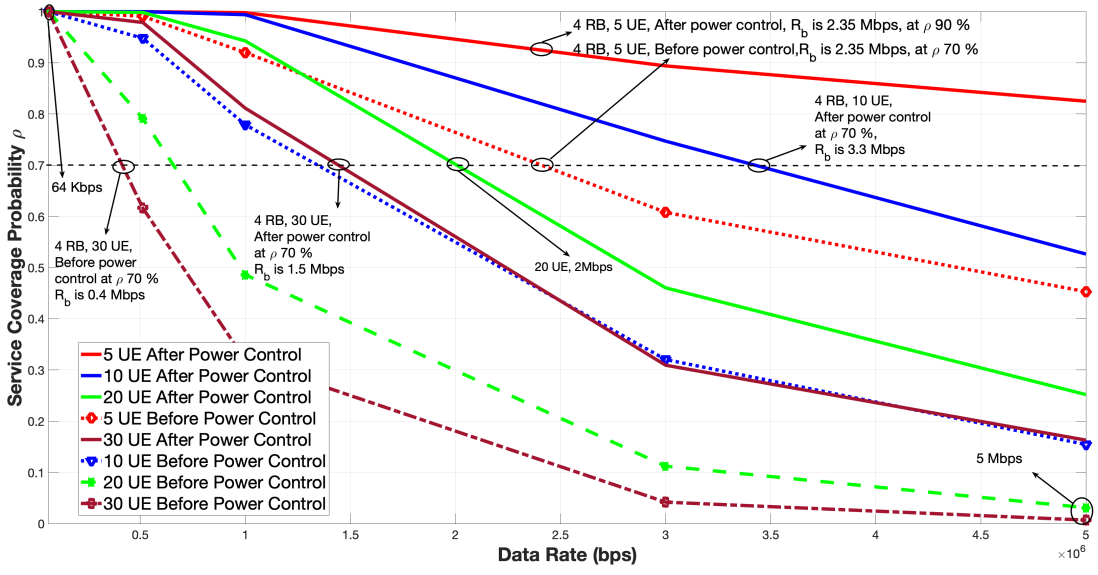

Figure 4.23: One cell special case: Service coverage probability versus the data rate with 4 RBs per UE, $R_b = 5$ Mbps. The analysis is for the data rate values after power control.

Also, comparing Fig. 4.21 with Fig. 4.23, the results show the same trend just as

in Fig. 4.20 and Fig. 4.21. As the number of RB per UE increases, the achievable data rate and service coverage probability increases. Interestingly, from Fig. 4.20 with 20 UEs at 70% coverage probability after power control, the achievable data rate 512 kbps, while from Fig. 4.22 with 20 UEs at 70% coverage probability after power control offers achievable data rate of 430 kbps. Also, with 60 UEs at 70% coverage probability after power control, 250 kbps is the achievable data rate in both Fig. 4.20 and Fig. 4.22. Since there is only 1 RB per UE, there is a higher SINR requirement, with higher transmit power requirement, which builds up the interference signal.
Moreover, from Fig. 4.21, with 10 UEs at 70% service coverage after power control, the achievable data rate is 3.8 Mbps, while with 20 UEs at the same benchmark, the achievable data rate is 2.2 Mbps. Conversely, Fig. 4.23 shows that with 20 UEs at 70% service coverage after power control, the achievable data rate is 2 Mbps and with 10 UEs at 70% service coverage after power control, the achievable data rate is 3.3 Mbps. Although, the RBs per UE is 4 and the SINR requirement is much lower, the interference between the access and backhaul links limits the achievable data rates. The interference is expected to scale up as the number of concurrent UEs within the cell increases.

4.7 Comparison between IAB and non-IAB Network

In Fig. 4.24, we show the service coverage probability for a non-IAB network, i.e., the cases with no SBS. Here, the results are presented for the cases with 4 RBs per UE with varying baseline data rates.

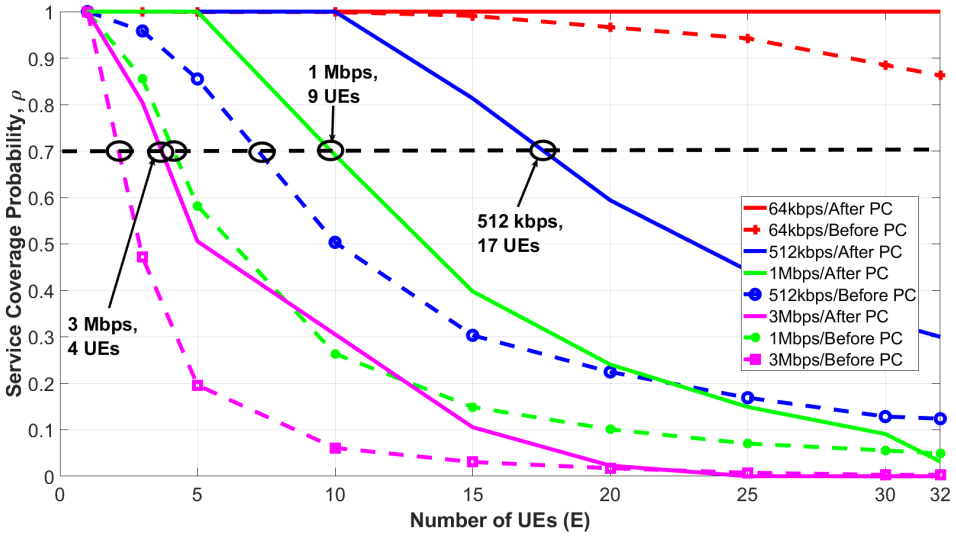

Figure 4.24: One cell: Service coverage probability versus the number of UEs, with 4 RB per UE, E =32, in non-IAB network.

Here, the result is compared with Fig. 4.6. The comparison shows that there is a possibility of having better service coverage probability with IAB networks than with non-IAB networks. From Fig. 4.24, at 70% service coverage probability with 3 Mbps baseline data rate, only 3 UEs are satisfied, versus 13 UEs, as seen in Fig. 4.6, after power control. Also, a steady decline in service coverage probability started just after the first UE is introduced into the cell in Fig. 4.24, while a decline started after 6 UEs are introduced randomly into the cell, for the same baseline data rate of 3 Mbps after power control in Fig. 4.6.

Interestingly, considering 3 Mbps as the baseline data rate, it is observed that with 25 UEs, before and after power control gives a zero service coverage probability for the non-IAB network. Meanwhile, with the modeled IAB network, the service coverage probability with 25 UEs, after power control, is about 40%. Thus, a well-planned and deployed IAB networks, with power control, may offer a better service coverage, compared to non-IAB networks.

4.8 Determination of the Effective Cell Radius

One of the parameters being optimized in IAB networks is the service coverage area. The service coverage area is directly related to the cell radius of the MBS. Our model is initially built on a cell radius of 200 m. In this test case, the cell radius is increased step-wise to 700 m. The simulation tries to observe the radius of the cell at which the service coverage probability starts to decline or shows a flat profile. Figure 4.25 shows the results.

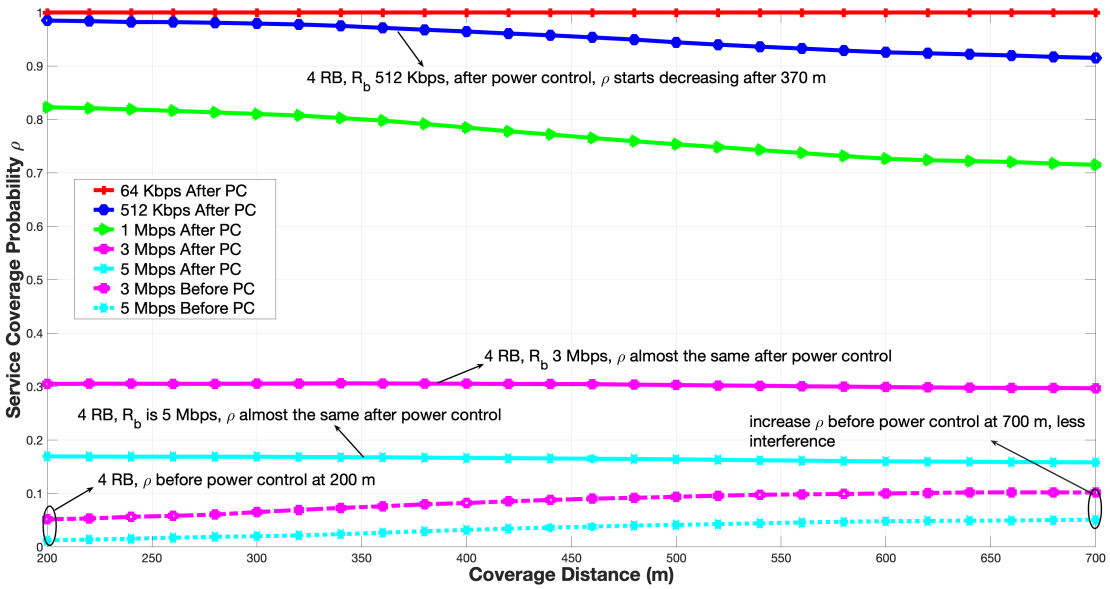

Figure 4.25: One cell: Service coverage probability versus increasing cell radius, with 4 RBs per UE, from 200 m to 700 m ($E = 32$).

The results show that before power control, there was a slight increase in the service coverage probability. The slight increase may be attributed to a reduction in

interference between UEs as the distance between the UEs increases, since there is a fixed number of UEs within the cell and they transmit at the same power of 23 dBm. With 64 kbps baseline data rate, both before and after power control, with increasing cell radius, the service coverage probability is the same. Furthermore, it is observed that by increasing the radius from 300 m to 400 m, the service coverage probability starts to decline and flatten out in other test cases. The observation may relate to the fact that the UEs at the edge of the cell are already transmitting at their maximum allowed transmit power and cannot do more than 43 dBm at this point. Knowing that the model uses mmWave which has short wavelength and short effective distance, it is seen that the service coverage probability within the cell starts to decrease after power control at around 300 m cell radius, for the same number of UEs randomly distributed.
Furthermore, the results from other tests related to inter-cell interference with two adjacent cells can be found in the appendix of our report, Appendix A. The results are other investigations about intra-cell and inter-cell interference in IAB networks.

4.9 Transmit Power Distribution of UEs

Here, the transmit power distribution of the UEs are analyzed. The cumulative distribution function (CDF) plot of the transmit powers shows the continuous distribution of the transmit powers for the UEs associated with the SBSs and the UEs associated with the MBS from a test case in Section 4.2. The CDF plot also shows the percentage of transmit power values of the UEs depending on the baseline service requirements. The CDF values range from the minimum to the maximum transmit powers proposed by 3GPP, [28].

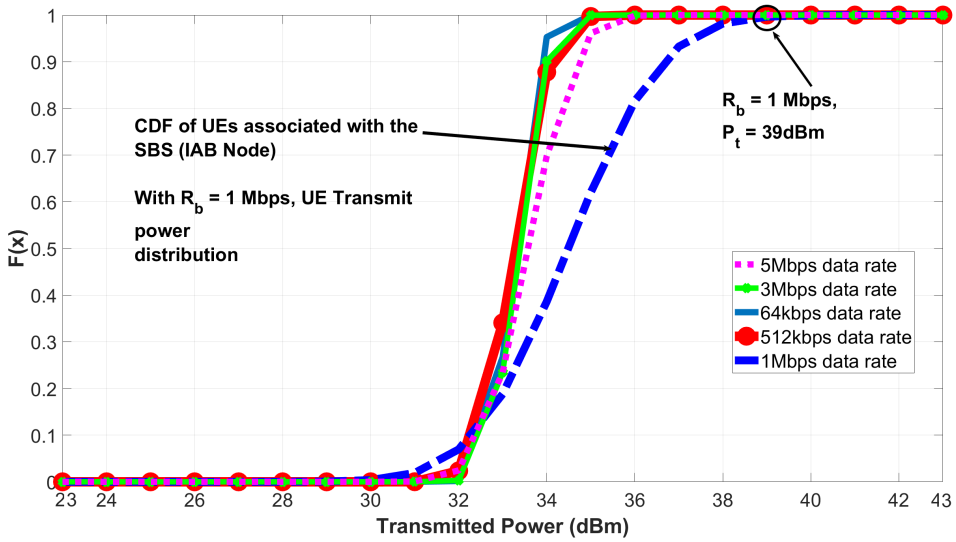

Figure 4.26: CDF for UEs associated with the SBS with fixed cell radius. The analysis is for the distribution of the transmit power values after power control.

From Fig. 4.26, derived from same data used in Section 4.2, it is observed that the distribution of the transmit powers reaches the CDF peaks between 35 dBm and 39 dBm. Here, there are 4 RBs allocated to each UE, with maximum of 32 concurrent UEs within the cell. Given a baseline of 1 Mbps, the transmit power peak starts from 39 dBm, which is the highest in all the test cases. Meanwhile, for lower data rates, 64 kbps and 512 kbps, the CDF peaks are at 35 dBm with lower distribution of transmit powers. Then, for 3 Mbps and 5 Mbps, have distribution more from 32 dBm to 36 dBm. As earlier established, the higher the data rate requirement, the higher the SINR requirement as well. For the UEs to have higher data rates, they need more transmit power and still need to operate with minimal interference.

From Eq.(3.12), it is obvious that data rate, R_b, and $SINR$ have a linear relationship, given a fixed bandwidth. Therefore, higher baseline data rate results in higher SINR requirement and more transmit power as well. With higher transmit power from the UEs, the interference within the cell increases and the service coverage probability reduces, meaning some UEs cannot meet the service requirements. The number of satisfied UEs reduces and the instant transmit power of the remaining satisfied UEs may reduce as well due to the GA final solutions, because interference will also reduce as some UEs dropped off. The change in power level and reduced number of UEs may be the reason why with 1 Mbps baseline data rate, there is a higher power distribution than with 3 Mbps or 5 Mbps test cases. Invariably, the number of satisfied UEs are more with 1 Mbps baseline data rate than with 3 Mbps and 5 Mbps test cases.

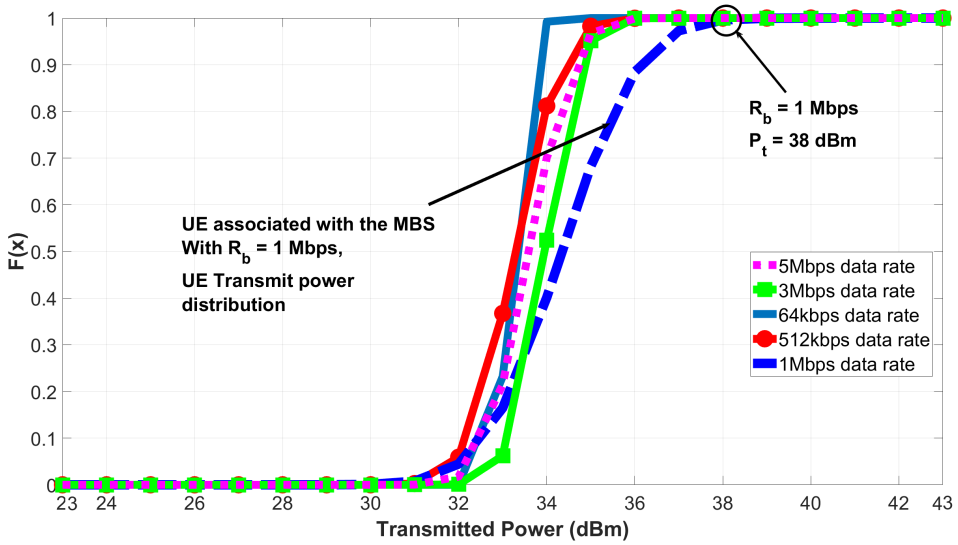

Figure 4.27: CDF for UEs associated with the MBS with fixed cell radius. The analysis is for the distribution of the transmit power values after power control.

From Fig. 4.27, it is observed that for the UEs associated with the MBS, the transmit power distribution is similar to what is seen in Fig. 4.26. Although, taking a look at 1 Mbps baseline data rate, the CDF reaches a peak at 38 dBm, which is 1

dBm less than the CDF of UEs associated with the SBS. There is a possibility of having more UEs associated with the SBS than with the MBS, which may increase the interference at the SBS. Then, the UEs transmit more power to meet the SINR requirement and to overcome the interference from other UEs.

Generally, comparing Fig. 4.26 and Fig. 4.27, it is observed that there is relatively the same transmit power distribution of all the UEs irrespective of their associated BS, either MBS or SBS, after power control. The results may point to the fact that power control tries to create a transmit power balance across all UEs within a cell, thereby improving the network capacity.

4.10 Convergence of the Genetic Algorithm

In all simulations, GA is used as a central daemon to offer fair power allocation values to the respective UEs and SBSs in uplink communication. The GA converged in all cases but at different iteration counts. Figure 4.28 shows the convergence of the GA from three simulations.

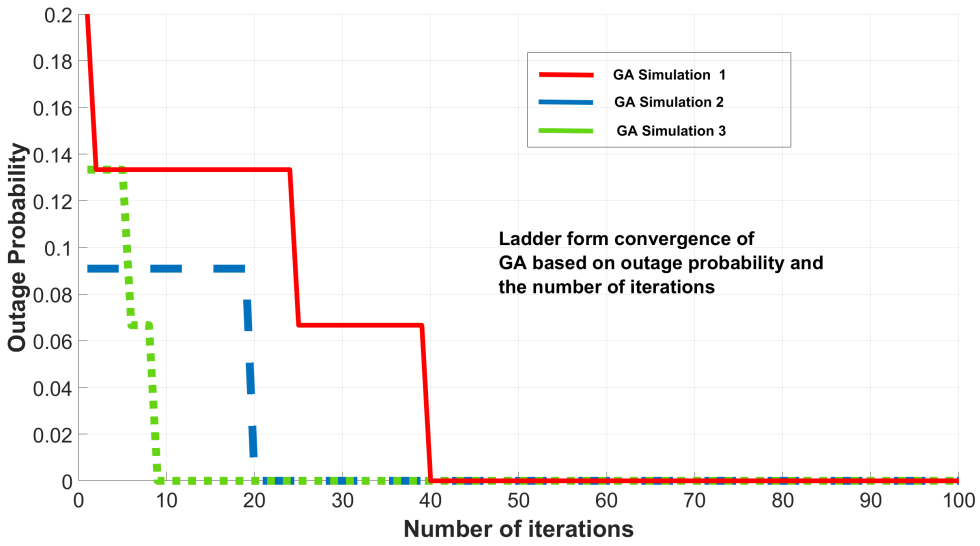

Figure 4.28: Plots of the convergence of Genetic Algorithm. Different GA convergence plots are captured for different simulations.

Specifically, as detailed in the Algorithm, we set $N = 200$, $K = 20$ and $S = 10$. As seen in Fig. 4.28, the algorithm converges in a ladder form. The observed ladder form is because using GA is not necessarily to find the best solution in every iteration, and it may be trapped in a local minimum. However, due to **Step 4** and **Step 6** of the Algorithm, GA can always avoid a local minimal and reach the global optimum if a sufficiently large number of iteration is considered, [39]- [42]. In GA, the larger the value of N, the more accurate the final solutions but at a cost of the iteration time. The higher the value of N, the slower the time taken for the algorithm to offer proper final solutions. Mostly, there is a trade-off between speed

and accuracy in iterative algorithms.

Also, it should be noted that the GA is independent of the channel model and so it can be applied in different channel models, [39]- [42]. From the results provided in our work, the GA offered a power control solution which could improve the service coverage probability of IAB networks. In all test cases, GA offers reasonable solutions for our multi-objective problem formulation.

5
Conclusion

This work investigated the performance of an IAB network using 3GPP proposed parameters. Particularly, we studied the effect of uplink power control on the service coverage probability of two-hop IAB network. For this reason, we developed a GA-based scheme for power control, and studied the effect of different parameters on the network performance. Our work considered a 28 GHz band for 5G deployment with TDD. We considered a finite number of resource blocks that a BS can offer in 5G. The model set-up had a cell radius of 200 m from the MBS. The UEs were randomly distributed per iteration to mimic the mobility. The pathloss was modeled using the 3GPP UMa model, putting into consideration the height of a MBS, SBSs, and UEs respectively. Also, fading, shadowing, and effects of rain were added to the overall channel loss. The EIRP values of the UE transmit power, as suggested by 3GPP, were used in the simulations. The baseline received SINR value was set to guarantee a target uplink data rate and assumed uncoded transmission. The power control solution was based on GA, implemented as a central daemon in the RAN. Signal interference seems to be a challenge that may limit the service coverage probability of IAB networks.

Based on the simulations carried out and our further analysis, it is observed that for effective control and minimization of interference, in TDD context, there should be a separation in time between the access and backhaul links. Without this, there is a possibility to increase the interference within the cell to an extent that the UEs will not have enough transmit power again to overcome the signal interference for a given baseline service requirement.

Moreover, with an increase in the allocated RBs per UE, or the UE operating bandwidth, there is a high possibility for better service coverage probability and higher data rates, at a cost of reduced number of concurrent UEs. Based on our models, the effect of inter-cell interference is minimal with a MBS cell of $>$ 200 m radius, operating at 28 GHz band, and channel bandwidth of 400 MHz. It is observed that, for the considered parameter setting, the effective cell radius is in between 300 m to 400 m.

Interestingly, the GA gives a proper power control to the transmit signal in terms of fairness and speed as an iterative power allocation scheme, which usually needs more time to converge. In most cases, the GA converges in less than 50 iterations. As demonstrated in all cases, a well-designed and implemented uplink power control scheme may improve service coverage probability in some cases within the IAB networks. Also, there is a possibility of having a better service quality with IAB networks as compared to non-IAB networks.

6
Future Works

Interestingly, the thesis work studied uplink power control in 5G IAB network under some defined conditions. It offers some logical conclusions into what must be put into perspective when deploying a 5G IAB network with the wireless channel bandwidth being shared between the access and backhaul links. Furthermore, the work also gives insight into some other areas that should be considered for future works, which will eventually lead to an all-encompassing IAB network solution. These includes:

- Identify a workable solution for load-balancing the UEs or traffic within an IAB network. Preferably, some IAB nodes, or BSs, should have a high cell load while others have less, based on the instantaneous quality of the backhaul links and the number of associated UEs. Having an appropriate distribution of the traffic load across all the BSs will help to avoid backhaul congestion.
- Investigate on combining power control and rate adaptation in the IAB uplink communication. The work may give insight into the variations of data rates that the UEs can have in uplink communication.
- Investigate the effect of edge computing and data storage capability of the IAB nodes on the QoS and QoE of the UEs.
- Identify and compare different efficient algorithms for resource allocation, including distributed power control schemes.
- Modelling massive MIMO for MBSs and SBSs, with beamforming capability, in uplink communication.
- Investigate the use of digital coding techniques in the massive MIMO use cases to control, or reduce, the effect of signal interference.

Bibliography

[1] V. Sahin, C. G. Omidyar and T. M. Bauman, "Telecommunications management network (TMN) architecture and interworking designs," in IEEE Journal on Selected Areas in Communications, vol. 6, no. 4, pp. 685-696, May 1988.

[2] K.Flynn, 2020. 5G for Industry 4.0. [online] 3gpp.org. Available at: https://www.3gpp.org/news-events/2122-tsn_v_lan [Accessed 5 June 2021].

[3] Y. Yang, K. W. Sung, L. Wosinska and J. Chen, "Hybrid fiber and microwave protection for mobile backhauling," in IEEE Wireless Commun. Lett./OSA Journal of Optical Communications and Networking, vol. 6, no. 10, pp. 869-878, Oct. 2014.

[4] L. Ma, X. Wen, L. Wang, Z. Lu and R. Knopp, "An SDN/NFV based framework for management and deployment of service based 5G core network," in China Communications, vol. 15, no. 10, pp. 86-98, Oct. 2018.

[5] S. Ahmadi, 2019. 5G NR. 1st ed. London: Academic Press, Elsevier Inc., pp.1 - 56, 254, 371-373, 380-400.

[6] Ericsson. Mobile Data Traffic Growth Outlook. Accessed: Jun. 5, 2021. [Online]. Available: https://www.ericsson.com/491e34/assets/local/mobility-report/documents/2018/ericsson-mobility-report-november-2018.pdf

[7] A. Goldsmith, 2005. Wireless communications. Cambridge: Cambridge University Press, pp.77-78, 293-315, 466-494, 505-528.

[8] S. Sreekumar, B. K. Dey and S. R. B. Pillai, "Distributed rate adaptation and power control in fading multiple access channels," in IEEE Trans. Inf. Theory, vol. 61, no. 10, pp. 5504-5524, Oct. 2015.

[9] C. Madapatha, 2020. Integrated access and backhaul for 5G and beyond. Master's Thesis. [online] Gothenburg: Chalmers University of Technology, pp.5-24.

[10] C. Madapatha, B. Makki, C. Fang, O. Teyeb, E. Dahlman, M. Alouini, T. Svensson. "On integrated access and backhaul networks: current status and potentials," in IEEE Open Journal of the Communications Society, vol. 1, pp. 1374-1389, 2020.

[11] M. Polese, M. Giordani, A. Roy, S. Goyal, D. Castor and M. Zorzi, "End-to-End simulation of integrated access and backhaul at mmWaves," in Proc. IEEE CAMAD'2018, Barcelona, Spain, 2018, pp. 1-7.

[12] A. Łukowa, V. Venkatasubramanian, E. Visotsky and M. Cudak, "On the coverage extension of 5G millimeter wave deployments using integrated access and backhaul," in Proc. IEEE PIMRC'2020, London, United Kingdom, 2020, pp. 1-7.

[13] E. Lagunas, L. Lei, S. Maleki, S. Chatzinotas and B. Ottersten, "Power allocation for in-band full-duplex self-backhauling," in Proc. IEEE TSP'2017, Barcelona, Spain, 2017, pp. 136-139.

[14] O. Teyeb, A. Muhammad, G. Mildh, E. Dahlman, F. Barac and B. Makki, "Integrated access backhauled Networks," in Proc. IEEE VTC'2019, Honolulu, HI, USA, 2019, pp. 1-5.

[15] M. Gupta, A. Rao, E. Visotsky, A. Ghosh and J. G. Andrews, "Learning link schedules in self-backhauled millimeter wave cellular networks," in IEEE Transactions on Wireless Communications, vol. 19, no. 12, pp. 8024-8038, Dec. 2020.

[16] C. Madapatha, B. Makki, A. Muhammad, E. Dahlman, M. Alouini, T.Svensson, "On topology optimization and routing in integrated access and backhaul networks: A Genetic Algorithm-based Approach", arXiv preprint arXiv:2102.07252, Feb. 2021. [Online]. Available: https://arxiv.org/pdf/2102.07252.pdf.

[17] H. Guo, B. Makki, D. Phan-Huy, E. Dahlman, M. Alouini, T. Svensson., "Predictor Antenna: A Technique to Boost the Performance of Moving Relays", arXiv preprint arXiv:2012.10537, May 2021.[Online]. Available: https://arxiv.org/pdf/2012.10537.pdf

[18] C. Fang, C. Madapatha, B. Makki, T.Svensson, "Joint scheduling and throughput maximization in self-backhauled millimeter wave cellular networks", arXiv preprint arXiv:2106.02570, Jun. 2021. [Online]. Available: https://arxiv.org/pdf/2106.02570.pdf.

[19] T. Inoue, "5G NR Release 16 and millimeter wave integrated access and backhaul," 2020 IEEE Radio and Wireless Symposium (RWS), San Antonio, TX, USA, 2020, pp. 56-59.

[20] GSMA, 2019. 5G Implementation Guidelines. [online] Gsma.com. Available at: https://www.gsma.com/futurenetworks/wp-content/uploads/2019/03/5G-Implementation-Guideline-v2.0-July-2019.pdf. pp.16-18.

[21] S. Nagul, "A review on 5G modulation schemes and their comparisons for future wireless communications," in Proc. IEEE SPACES'2018, Vijayawada, India, 2018, pp. 72-76.

[22] J. Navarro-Ortiz, P. Romero-Diaz, S. Sendra, P. Ameigeiras, J. J. Ramos-Munoz and J. M. Lopez-Soler, "A survey on 5G usage scenarios and traffic models," in IEEE Communications Surveys Tutorials, vol. 22, no. 2, pp. 905-929, Second quarter 2020.

[23] Y. Takahashi, K. Muraoka, J. Mashino, S. Suyama and Y. Okumura, "5G Downlink throughput performance of 28 GHz band experimental trial at 300 km/h," in Proc. IEEE PIMRC'2018, pp. 1140-1141.

[24] R. Tian, K. Senda and H. Otsuka, "BER performance of OFDM-based 4096-QAM using soft decision Viterbi decoding in multipath fading," in Proc. IEEE WSCE'2018, Singapore, pp. 1-4.

[25] M. N. Islam, S. Subramanian and A. Sampath, "Integrated access backhaul in millimeter wave networks," in Proc. IEEE WCNC, 2017, pp. 1-6.

[26] A. Zaidi, F. Athley, J. Medbo, U. Gustavsson, G. Durisi, and X. Chen, 2018. 5G physical layer. 1st ed. London: Academic Press, pp.23-64.

[27] G. Barb, M. Otesteanu, F. Alexa and F. Danuti, "OFDM multi-numerology for future 5G New Radio communication systems," in Proc. IEEE SoftCOM'2020, Split, Croatia, 2020, pp. 1-3.

[28] 3GPP TS 38.101-2 V17.1.0 (2021-03) NR;User Equipment (UE) radio transmission and reception; Part 2: Range 2 Standalone (Release 17). Available at: https://www.3gpp.org/ftp/Specs/archive/38_series/38.101-2/

[29] Nokia, 2020. Looking for faster 5G mmWave rollout?. [image] Available at: https://www.nokia.com/blog/looking-for-faster-5g-mmwave-rollout-find-out-how-iab-will-help/

[30] J. Kim, I. Kim and H. Chung, "Resource multiplexing enhancements for integrated access and backhaul in 5G New Radio Release 17," in Proc. IEEE ICTC'2020, pp. 936-938.

[31] H. Ronkainen, J. Edstam, A. Ericsson, and C. Östberg, 2020. Introducing Integrated Access and Backhaul. Ericsson Technology Review, [online] (ISSN 0014-0171 284 23-3346), pp.4-7. Available at: https://www.ericsson.com/49e6f6/assets/local/reports-papers/ericsson-technology-review/docs/2020/introducing-integrated-access-and-backhaul.pdf

[32] R. Dilli, "Analysis of 5G wireless systems in FR1 and FR2 frequency bands," in Proc. IEEE ICIMIA'2020, pp. 767-772.

[33] 3GPP TR 38.901 V16.1.0 (2019-12) Study on channel model for frequencies from 0.5 to 100 GHz (Release 16). Available at:https://www.3gpp.org/ftp/Specs/archive/38_series/38.901/

[34] J. Huang, Y. Cao, X. Raimundo, A. Cheema and S. Salous, "Rain statistics investigation and rain attenuation modeling for millimeter wave short-range fixed links," in IEEE Access, vol. 7, pp. 156110-156120, 2019.

[35] ITU-R Recommendation P.838-3. 'Specific attenuation model for rain for use in prediction methods', International Telecommunication Union, 2006. Available at: https://www.itu.int/dms_pubrec/itu-r/rec/p/R-REC-P.838-3-200503-I!!PDF-E.pdf

[36] 3GPP TS 38.300 V16.2.0 (2020-07) Technical Specification Group Radio Access Network;NR; NR and NG-RAN Overall Description;Stage 2(Release 16). Available at:https://www.3gpp.org/ftp/Specs/archive/38_series/38.300/

[37] K. Ulaganathen, A. R. Tharek, R. M. Islam and K. Abdullah, "Rain attenuation for 5G network in tropical region (Malaysia) for terrestrial link,"in Proc. IEEE MICC'2017, pp. 35-38.

[38] G. R. MacCartney and T. S. Rappaport, "Millimeter-wave base station diversity for 5G coordinated multipoint (CoMP) applications," in IEEE Transactions on Wireless Communications, vol. 18, no. 7, pp. 3395-3410, July 2019.

[39] B. Makki, A. Ide, T. Svensson, T. Eriksson and M. Alouini, "A genetic algorithm-based antenna selection approach for large-but-finite MIMO networks," in IEEE Transactions on Vehicular Technology, vol. 66, no. 7, pp. 6591-6595, July 2017.

[40] B. Makki, T. Svensson and M. Alouini, "On the throughput of large-but-finite MIMO networks using schedulers," in IEEE Trans. Wireless Commun., vol. 18, no. 1, pp. 152-166, Jan. 2019.

[41] H. Guo, B. Makki and T. Svensson, "A genetic algorithm-based beamforming approach for delay-constrained networks," in Proc. IEEE WiOpt'2017, pp. 1-7.
[42] B. Makki, T. Svensson, G. Cocco, T. de Cola and S. Erl, "On the throughput of the return-link multi-beam satellite systems using genetic algorithm-based schedulers," in Proc. IEEE ICC'2015, pp. 838-843.

A

Appendix 1

A.1 Inter-cell Distance and Inter-cell Interference

By increasing the inter-cell distance, we may observe some effects of inter-cell interference. This set-up shows only about 1% improvement in the service coverage probability, after power control. Empirically, it is taken therefore that the interference from adjacent cells is quite minimal. This is inferred from figure A.1.

Note: The operating frequency band is 28 GHz with a cell radius of 200 m and 32 UEs only.

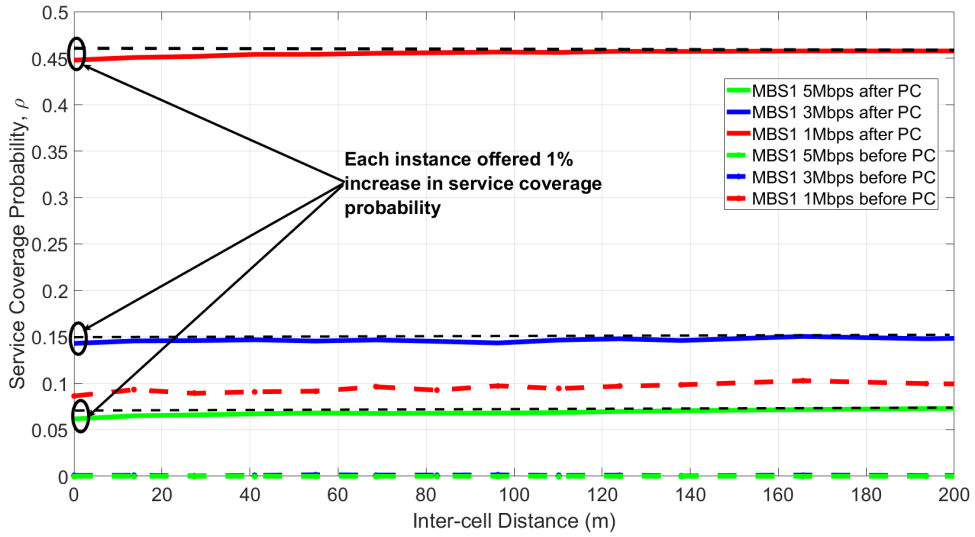

Figure A.1: Service coverage probability versus inter-cell distance. Here, only two adjacent cells are used for the test, the distance between two cells start for 0 to 200 m, $E = 4$, $RB = 2$ per UE, $E = 32$.

A.2 Intra-cell Distance and Intra-cell Interference

Also, by increasing the cell radius, we may observe a trend in the service coverage probability. It is observed that the service coverage probability, after power control, starts to decline at distances between 300 m and 400 m, depending on the baseline data rate and RB.

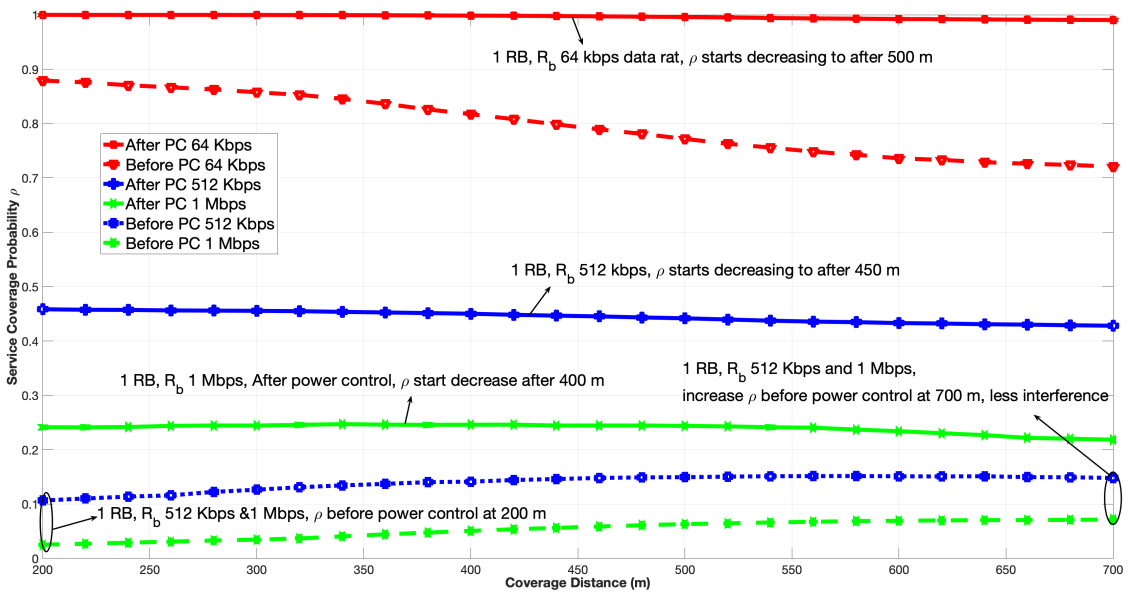

Figure A.2: Service coverage probability versus intra-cell distance, r = (200 m to 700 m), with 1 RB per UE, $E = 32$, $M = 4$.

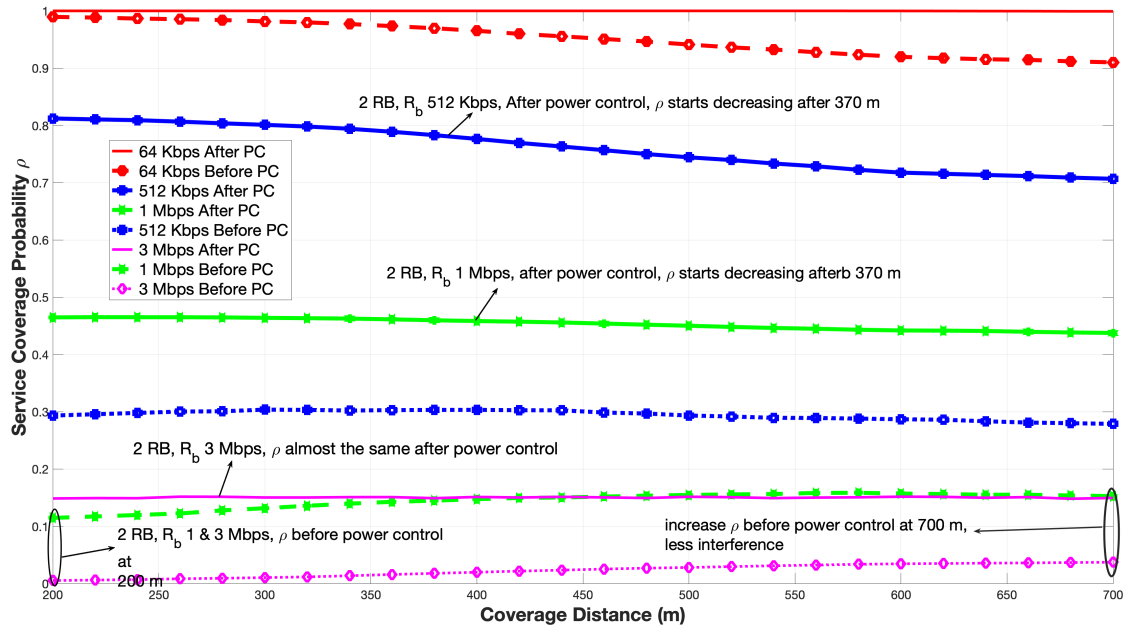

Figure A.3: Service coverage probability versus intra-cell distance, r = (200 m to 700 m), with 2 RBs per UE, $E = 32$, $M = 4$.

DEPARTMENT OF SOME SUBJECT OR TECHNOLOGY
CHALMERS UNIVERSITY OF TECHNOLOGY
Gothenburg, Sweden
www.chalmers.se

CHALMERS
UNIVERSITY OF TECHNOLOGY